Original Research Article

Improving fatty liver hemorrhagic syndrome in laying hens through gut microbiota and oxylipin metabolism by *Bacteroides fragilis:* A potential involvement of arachidonic acid

Shaobo Zhang [a], Manhua You [a], Youming Shen [b], Xinghua Zhao [a], Xin He [a], Juxiang Liu [a], Ning Ma [a, *]

[a] *College of Veterinary Medicine, Veterinary Biological Technology Innovation Center of Hebei Province, Hebei Agricultural University, Baoding 071001, China*
[b] *Research Institute of Pomology, Chinese Academy of Agricultural Sciences, Xingcheng 125100, China*

A B S T R A C T

Bacteroides fragilis (*B. fragilis*), a crucial commensal bacterium within the gut, has shown connections with hepatic lipid metabolism and inflammation regulation. Nonetheless, the role of *B. fragilis* in the progression of fatty liver hemorrhagic syndrome (FLHS) remains unknown. This study aims to explore the ameliorative effects of *B. fragilis* on FLHS in laying hens, as well as its underlying mechanisms. This is the first study to employ a chicken FLHS model, combining microbiomics and oxylipin metabolomics to investigate the mechanism of action of intestinal symbiotic bacteria. Exp. 1: 40 laying hens at 25 weeks old were randomly divided into five treatment groups (eight replicates per group and one hen per replicate), including the control group (basal diet), the high-energy and low-protein (HELP) group, and the HELP group with three different levels (10^8, 10^9, and 10^{10} CFU) of *B. fragilis*. Exp. 2: 18 chickens at 25 weeks old were randomly divided into three treatment groups (six replicates per group and one hen per replicate) including the control group (basal diet), the model group (HELP diet), and the arachidonic acid (AA) group (HELP diet with 0.3% AA). The experiment period of Exp. 1 and Exp. 2 were 8 weeks. *B. fragilis* significantly improved body weight of seventh week ($P = 0.006$), liver lipid degeneration, blood lipid levels (triglycerides, cholesterol, and low-density lipoprotein cholesterol; $P < 0.05$), and liver function (alanine aminotransferase and aminotransferase; $P < 0.05$) in laying hens. *B. fragilis* downregulated the expression of lipid synthesis-related genes fatty acid synthase, acetyl-CoA carboxylase, and liver X receptor α, and inflammation-related genes tumor necrosis factor α, interleukin (*IL*)-1β, *IL-6*, and *IL-8* in the liver of FLHS-affected hens ($P < 0.05$), while upregulating the expression of lipid oxidation-related genes carnitine palmitoyl transferase-1, peroxisome proliferator activated receptor (*PPAR*) α, and *PPARγ* ($P < 0.05$). The in-depth analysis indicated alterations in oxylipin pathways triggered by *B. fragilis*, as evidenced by changes in the expression of pivotal genes arachidonate 15-lipoxygenase, arachidonate 5-lipoxygenase ($P < 0.05$), subsequently causing modifications in relevant metabolites. This included a decrease in pro-inflammatory substances such as 15-oxoETE ($P = 0.004$), accompanied by an increase in AA ($P = 0.008$). *B. fragilis* regulated the homeostasis of intestinal flora by increasing the abundance of *Bacteroides* and decreasing the abundance of *Succinatimonas* and *Faecalicoccus* ($P < 0.05$). The integrated analysis revealed a robust positive correlation between *Bacteroides* abundance and AA levels ($P = 0.007$). This relationship was corroborated through in vitro experiments. Subsequently, the beneficial effect of AA in mitigating FLHS was confirmed in laying hens with FLHS, further supported by reverse transcription-polymerase chain reaction analysis demonstrating gene expression patterns akin to

B. fragilis intervention. This study demonstrated that *B. fragilis* exerts an anti-FLHS effect through modulation of oxylipin metabolism and gut microbiota stability, with a pivotal role played by AA.

1. Introduction

Nonalcoholic fatty liver disease (NAFLD) is a complex and pervasive metabolic disorder that plagues a substantial proportion of the global population (Byrne and Targher, 2015; Targher et al., 2021). Characterized by the buildup of triglycerides (TG) in hepatocytes, NAFLD is caused by the excessive and unwarranted accumulation of lipids in the liver, which triggers the development of hepatic steatosis. As the disease progresses, NAFLD inflicts inflammation and fibrosis in the liver and eventually leads to cirrhosis and liver cancer. Currently, the prevailing model organisms for studying NAFLD are rodents, particularly rats and mice. Comparative physiology reports have shown that adipose tissue and liver are almost equally responsible for de novo lipogenesis (DNL) in rodents (Hamid et al., 2019). Conversely, laying hens afflicted with fatty liver hemorrhagic syndrome (FLHS) closely resemble humans with NAFLD, as their liver primarily contributes to DNL (G Gao et al., 2021), which makes them a suitable model for investigating human lipid metabolism disorders. As such, leveraging the use of laying hens presents a novel and promising opportunity to advance the understanding of the pathophysiology of NAFLD and explore potential therapeutic interventions.

The intestinal flora represents a highly intricate microbial community residing in the digestive tract of both humans and animals, and its association with host metabolic diseases has been proven. Perturbations in the composition and function of the intestinal flora can profoundly affect the onset and progression of FLHS (Hamid et al., 2019; Li et al., 2020). Specifically, FLHS-affected hens exhibit a decline in the abundance of *Bacillus mimicus*, *Bacteroides*, and *Lactobacillus*, alongside an increase in *Desulfovibrio*, *Clostridium tansy*, and *Enterococcus faecalis* in the gut (Liu et al., 2022). In contrast, healthy hens harbor gut microbiota featuring bacteria that impede host energy absorption or promote intestinal health (Li et al., 2020). Impaired intestinal barrier function, increased intestinal permeability, altered bile acid metabolism, and endotoxin-activated hypo-inflammation are all linked to the disrupted intestinal flora, which are involved in the development and progression of FLHS. Consequently, rectifying intestinal microbial homeostasis represents a crucial approach to preventing and treating FLHS. In our previous study, a disruption of the cecum flora in diseased hens was accompanied by a significant decrease in the abundance of *Bacteroides* compared to healthy hens (Liu et al., 2022). Wu et al. (2022) reported similar findings, demonstrating a 13% reduction in the abundance of Bacteroidetes and a 6.6% decrease in the abundance of the *Bacteroides* genus in the ileum of FLHS hens compared to healthy hens. Additionally, research has shown that hens fed rapeseed meal-induced hepatic steatosis and cholesterol (TC) deposition experienced a significant decrease in the abundance of the *Bacteroides* genus (Zhu et al., 2021). Therefore, it is speculated that FLHS may be related to the decrease in the abundance of *Bacteroides*.

Bacteroides is a dominant species of intestinal commensal bacteria, and recent research has highlighted its potential for improving metabolic disorders such as NAFLD. For instance, *Bacteroides xylanisolvens* may improve NAFLD through its metabolite folic acid, which enhances folic acid-dependent single-carbon metabolism, increases the antioxidant capacity of the liver, and improves abnormal lipid metabolism (Qiao et al., 2020). Another study on *Parabacteroides distasonis* found that this species reduced hyperglycemia in mice by activating intestinal gluconeogenesis through the secretion of succinate. Furthermore, *P. distasonis* altered the composition of intestinal bile acids, activated the farnesoid x receptor-fibroblast growth factors 15 signaling pathway, and enhanced the integrity of the intestinal barrier, thereby reducing hyperlipidemia (Wang et al., 2019). Arachidonic acid (AA) is a polyunsaturated fatty acid that is widely distributed in living organisms. By adding 1% AA to the diets of mice on a high-fat diet, Zhuang et al. (2017) found that AA could affect the gut—hypothalamus—liver axis in a sex-dependent manner, thereby improving obesity and NAFLD. Several studies have reported the presence of AA metabolism disorder with reduced AA levels in NAFLD (Gai et al., 2018). AA is metabolized by the cyclooxygenase, lipoxygenase (LOX), and cytochrome P450 enzyme pathways to produce biologically active metabolites such as prostaglandins, leukotrienes, and epoxyeicosatrienoic acids. These metabolites play a role in inflammation, lipid metabolism, and other processes through specific receptors (Meng et al., 2021). Recently, studies have found that *Bacteroides fragilis* (*B. fragilis*) could secrete AA to alleviate hypersaline hypertension and Alzheimer's disease caused by reduced AA levels (Chen et al., 2022; Yan et al., 2020). Based on the previous findings of AA metabolism disorder and reduced AA concentration in FLHS laying hens, it is reasonable to presume that *B. fragilis* may play a role in the FLHS disease process through AA metabolism.

Oxylipin metabolomics is a cutting-edge analytical technique within the realm of lipidomics, aimed at investigating a diverse range of biologically active lipid molecules, particularly encompassing omega-3 and omega-6 fatty acids and their derivatives such as prostaglandins, leukotrienes, and various other compounds (Barquissau et al., 2017). Through oxylipin metabolomics, a comprehensive understanding of lipid signaling pathways, inflammatory regulation, oxidative stress responses, and intricate networks of metabolic disruptions can be achieved (Rohwer et al., 2023). The intestinal microbiota is a key factor affecting systemic metabolism, and the cecum microbes associated with FLHS can alter various pathways such as energy harvesting, insulin resistance, and lipid metabolism in the host. However, until now, few studies have reported that oxylipins interact with intestinal flora to affect liver lipid metabolism. Therefore, the microbiome combined with oxylipin metabolomics can provide a new window for the study of FLHS.

Based on previous research and existing reports, we hypothesize that cecal *Bacteroides* plays an important role in FLHS, possibly participating in the process by diving oxylipin metabolism. In this study, we initially isolated a novel strain of *B. fragilis* from the cecum of laying hens and investigated its effect on FLHS by assessing relevant clinical parameters. Subsequently, employing 16S rRNA sequencing and oxylipin metabolomics techniques, we examined the influence of this strain on gut microbiota composition and oxylipin metabolism. Correlation analysis, combined with in vitro cultivation of *B. fragilis*, revealed a potential link between this bacterium and AA. Furthermore, through the addition of AA to

the diet, we confirmed its beneficial role in mitigating FLHS in laying hens. Reverse transcription-polymerase chain reaction (RT-PCR) analysis demonstrated similarities in the effects of AA and *B. fragilis*. These findings provide a basis for the potential application of *B. fragilis* in laying hens affected with FLHS and offer valuable insights into its role in NAFLD.

2. Materials and methods

2.1. Animal ethics statement

This animal experiment was reviewed and approved by the Animal Care and Use Committee of Hebei Agricultural University (No. 2023179) (Baoding, China).

2.2. Bacterial strains and culture conditions

The bacterial strain utilized in this study was isolated from the cecal content of healthy laying hens. By comparing its 16S rRNA gene sequence to the NCBI reference database (https://www.NCBI.nlm.nih.gov/), the strain was identified as *B. fragilis* (Fig. S1). The *B. fragilis* strain was cultured in anaerobically sterilized BHI medium containing 0.01% hemin, 0.01% vitamin K$_1$, and 0.01% L-cysteine (Qingdao Hi-Tech Industrial Park Hope Bio-Technology Co., Ltd., Shandong, China). Anaerobic culture was performed at 37 °C for 24 h. The bacterial culture medium was centrifuged at 8000 × *g* for 10 min at 4 °C. The bacterial sludge was then washed twice with sterile phosphate buffer solution and resuspended to 1 × 10^{10} CFU/mL for animal experiments.

2.3. Animal experiment

In this study, 40 healthy Jing Fen laying hens (1.56 ± 0.07 kg), aged 25 week, were used. The birds were randomly divided into five groups (8 replicates per group and 1 hen per replicate). The control group (Control) was fed a standard diet and vehicle, while the other four groups were fed a HELP diet to induce FLHS. The four groups received different types of feed, including vehicle, a low dose of *B. fragilis* suspension (LBF; 1 × 10^8 CFU), a medium dose of *B. fragilis* suspension (MBF; 1 × 10^9 CFU) and a high dose of *B. fragilis* suspension (HBF; 1 × 10^{10} CFU). The prepared oral live bacterial suspension was administered once daily gavage to the experimental laying hens for 8 weeks. FLHS was induced by the HELP diet as in previous studies (Liu et al., 2022; Meng et al., 2021). The composition and nutrient levels of the standard diet and HELP diet are presented in Table 1. Daily feed intake of laying hens was recorded. The birds were housed in a single room with a two-layer cage design, with two hens in each cage. The room temperature was maintained at 20 °C, and the hens received 16 h of light per day. Prior to conducting the experiment, the laying hens were subjected to a 2-week adaptation period. The formal experiment lasted for 8 weeks, during which the laying hens had ad libitum access to feed and water, and their body weights were measured weekly.

The determination of crude protein in feed followed the Chinese national standard (GB/T 6432−2018) using the Kjeldahl method. The automatic Kjeldahl nitrogen analyzer employed in this process was purchased from FOSS Company (Hilloeroed, Denmark). For the measurement of total phosphorus in feed, the spectrophotometric method as outlined in the Chinese national standard (GB/T 6437−2018) was employed. The sample preparation for the feed was carried out by dry ashing, followed by the addition of ammonium vanadomolybdate reagent for reaction. Subsequently, the absorbance is measured at 400 nm using a UV−visible spectrophotometer (SHIMADZU, Kyoto, Japan). The phosphorus content is then calculated by comparing the absorbance values to a standard

Table 1
Composition and nutrient levels of the standard diet and HELP diet (air-dry basis, %).

Item	Standard diet	HELP diet
Ingredients		
Corn	64.00	70.00
Wheat bran	2.00	1.20
Soybean meal (44% crude protein)	24.00	14.58
Fat-soybean oil		4.22
Calcium carbonate	8.00	8.00
Premix[1]	2.00	2.00
Total	100.00	100.00
Nutrient levels		
Crude protein[2]	15.80	12.30
Phosphorus[2]	0.54	0.51
Calcium[2]	3.55	3.53
Lysine[3]	0.96	0.69
Arginine[3]	1.03	0.74
Methionine[3]	0.37	0.32
Valine[3]	0.77	0.58
Metabolic energy, kcal/kg[3]	2679	3100
Methionine + cysteine[3]	0.67	0.56

HELP = high-energy and low-protein.

[1] The ingredient of premix per gram: VA 12,500 IU; VD$_3$ 32,500 IU; VE 18.75 mg; VK$_3$ 2.65 mg; VB$_1$ 2 mg; VB$_2$ 6 mg; VB$_{12}$ 0.025 mg; CaHPO$_4$ 500.00 mg; cupric sulfate 4.6 mg; ferrous sulfate 28.4 mg; manganous sulfate 35.46 mg; zinc sulfate 76 mg; zeolite powder 6 mg; sodium selenite 5 mg; anti-oxidizing quinolone 50 mg; choline 90 mg; bacitracin zinc 26.7 mg; methionine 100 mg.

[2] All data results were obtained through chemical analysis and were presented as the average of two measurements.

[3] The levels of amino acids and metabolic energy were calculated based on the Tables of Feed Composition and Nutritive Values in China (31st edition).

curve. Finally, the calcium content in the feed was determined according to the Chinese national standard (GB/T 6436−2018).

2.4. Sample collection

At the end of the 56-day experiment, all the hens were deprived of feed for 12 h. Afterward, blood samples were collected from the inferior pterygoid vein and kept temporarily on ice. Serum samples were obtained from the blood samples by centrifuging at 3000 × *g* for 10 min. The laying hens were also euthanized by the jugular vein for tissue collection. The whole livers of the hens were collected and weighed, and their relative weights were calculated using the formula:

Liver index (%) = [tissue organ weight (g)/body weight (g)] × 100.

A small part of the liver was sectioned and used for hematoxylin and eosin (H&E) and Oil Red O staining. A small piece of the liver was quenched in liquid nitrogen and frozen at −80 °C until it was used for oxylipin metabolomics analysis. The cecum was ligated at both ends, and the mid-cecum tissue and contents were collected separately in sterile, frozen storage tubes for the analysis of gut microbiota.

2.5. Biochemical and pathological analysis

The levels of TC, TG, high density lipoprotein cholesterol (HDL-C), low density lipoprotein cholesterol (LDL-C), aspartate aminotransferase (AST), and alanine aminotransferase (ALT) in serum were detected by a blood biochemical analyzer XL 640 (Erba, Mannheim, Germany). The steps of liver pathology are as follows. First, the liver was fixed, dehydrated, and sectioned (Oil Red O staining was performed using frozen sections). Subsequently, staining procedures were carried out following the instructions provided in the H&E and Oil Red O staining kits. Images were then captured under a microscope (Carl Zeiss AG, Oberkochen, Germany).

2.6. RT-PCR analysis of genes related to lipid metabolism and inflammation in the liver

Briefly, total RNA from tissues was extracted using the TaKaRa MiniBEST Universal RNA Extraction Kit (code No. 9796, TaKaRa Bio., Kyoto, Japan) and subsequently reverse transcribed to cDNA using the PrimeScript RT reagent Kit (Perfect Real Time, code No. RR047A, TaKaRa Bio., Kyoto, Japan). cDNA was reversed transcribed in gradient dilutions to determine the optimal concentration. The PCR reactions were then performed using TB Green Premix Ex Taq II (Tli RNaseH Plus, code No. RR420A, TaKaRa Bio., Kyoto, Japan), ROX plus and a Bio-Rad CFX Connect fluorescent quantitative PCR instrument (Hercules, CA, USA). The related mRNA expression was normalized to glyceraldehyde-3-phosphate dehydrogenase (*GAPDH*), and RT-PCR data were analyzed using the comparative $2^{-\Delta\Delta Ct}$ method. The identified genes were associated with various aspects of metabolism: lipid synthesis genes included acetyl-CoA carboxylase (*ACC*), fatty acid synthase (*FAS*), liver X receptor α (*LXRα*), and apical sodium-dependent bile acid transporter (*ASBT*); lipid oxidation genes encompassed peroxisome proliferator activated receptor (*PPAR*) α, *PPARγ*, and carnitine palmitoyl transferase-1 (*CPT-1*); and inflammation-related genes comprised tumor necrosis factor-α (*TNF-α*), interleukin (*IL*)-1β, *IL-6*, and *IL-8*. Details of the primers employed in the experiment are provided in Table 2.

2.7. Microbiomics analysis

Bacterial DNA wlas extracted from the contents of the cecum using a bacterial genomic DNA extraction kit (TianGen Biotech Co., Ltd., Beijing, China) following the manufacturer's instructions. Primers 341F (5′-ACTCCTACGGGRSGCAGCAG-3′) and 806R (5′-GGACTACVVGGGTATCTAATC-3′) were employed for PCR amplification of the 16S rRNA gene. The purified PCR products were sequenced on the NovaSeq 6000 (Illumina, CA, USA) platform with PE 250. The raw reads of the samples were assembled using FLASH (Version 1.2.11) to generate raw tags, which were then subjected to quality control using fastp software (Version 0.23.1) to obtain clean tags. The chimera sequences were eliminated by aligning the clean tags with the Silva database. The obtained data were processed using QIIME2 software for denoising, species annotation, and analysis of alpha diversity, beta diversity, and principal coordinate analysis (PCoA). Linear discriminant analysis effect size (LEfSe) analysis was performed using the microeco package (linear discriminant analysis score >2). Spearman correlation analysis was performed in R language to investigate the associations between differential bacteria and clinical indicators, as well as the correlations between differential bacteria and differential metabolites.

2.8. Oxylipin metabolism in liver

Sample pretreatment and LC-MS/MS conditions are shown in the supporting information methods. For qualitative analysis of the mass spectrometry data, a database constructed based on standard substances was used. The Analyst (Version 1.6.3) and MultiQuant (Version 3.0.3) software packages were employed for qualitative and quantitative analysis of the mass spectrometry data. Unsupervised principal component analysis (PCA) was conducted using the prcomp function in R (www.r-project.org). Cluster analysis, and orthogonal partial least squares discriminant analysis (OPLS-DA) were performed to analyze the overall samples. Based on the OPLS-DA results, metabolites showing significant differences were selected based on the variable importance in the projection (VIP) obtained from the multivariate analysis model (VIP >1). Differential metabolites were further screened using fold change (FC) analysis (FC ≤ 0.5, or FC ≥ 2). Subsequently, differential metabolites were

Table 2
Primers used for reverse transcription-polymerase chain reaction analysis.

Gene	Primer sequence (5' to 3')	Accession number
FAS	F: AAAGCAATTCGTCACGGACA R: GGCACCATCAGGACTAAGCA	NM_001114269.1
ACC	F: CCGAGAACCCAAAACTACCAG R: GCCAGCAGTCTGAGCCACTA	XM_038165892.1
LXRα	F: GACCTGAGCTATAATCGGGATG R: TCAGGTGATCATTTGGTCTGTTG	NM_204542.3
ASBT	F: TTATGCCTCTCACAGCCTTCTTGC R: TCCATGTCACCATCCACCCAGTAG	NM_001319027.1
CPT-1	F: GGAGAACCCAAGTGAAAGT R: TGGAAACGACATAAAGGCAGAA	XM_027457809.2
PPARα	F: TAACGGAGTTCCAATCGC R: AACCCTTACAACCTTCACAA	XM_038165892.1
PPARγ	F: CACTGCAGGAACAGAACAAAGAA R: TCCACAGAGCGAAACTGACATC	AJ250838
TNF-α	F: GAGCGTTGACTTGGCTGTC R: AAGCAACAACCAGCTATGCAC	HQ739087.1
IL-1β	F: ACTGGGCATCAAGGGCTA R: GGTAGAAGATGAAGCGGGTC	AJ245728
IL-6	F: AAATCCCTCCTCGCCAATCT R: CCCTCACGCTCTTCTCCATAAA	AJ250838
IL-8	F: ATGAACGGCAAGCTTGGAGCTG R: TCCAAGCACCTCTCTTCCATCC	HQ739083.1
PLA2G4	F: ACTTGACCACTTCCCGTGAC R: GGGTTGTGACTGACCGAGTT	NM_205423.1
ELOVL5	F: ATTGGGTGCCTTGTGGTCA R: AGCTGGTCTGGAAGATTGTCA	NM_001199197.2
FADS1	F: GGAAACAGTGGGTGGACCT R: AGATGAAGCCCCAGGATACC	XM_046919233.1
ALOX15	F: CTTTGGGGAGGTCTTTGC R: GCCAGCGTGTTGATGTGC	XM_033846983.1
ALOX5	F: GCGTGGATGCCAATAAGAC R: GAGACTAGGTGTGTCCGTAAGAG	XM_046920513.1
GPX4	F: AACCAGTTCGGGAAGCAGGA R: ACTTGATGGCATTCCCCAGC	NM_204220.3
HPGDS	F: TGGCAAAGTTCCTATTCTGG R: ATCCTGATTTTTCTCTGCCC	NM_205011.2
GAPDH	F: TGCTGCCCAGAACATCATCC R: ACGGCAGGTCAGGTCAACAA	NM_204305.1

FAS = fatty acid synthase; *ACC* = acetyl-CoA carboxylase; *LXRα*= liver X receptor α; *ASBT*= apical sodium-dependent bile acid transporter; *PPAR*= peroxisome proliferator activated receptor; *CPT-1*= carnitine palmitoyl transferase-1; *TNF-α*= tumor necrosis factor-α; *IL*= interleukin; *PLA2G4* = phospholipase A2 group IVA; *ELOVL5* = elongase of very-long fatty acid 5; *FADS1* = fatty acid desaturase 1; *ALOX15* = arachidonate 15-lipoxygenase; *ALOX5* = arachidonate 5-lipoxygenase; *GPX4* = glutathione peroxidase 4; *HPGDS* = hematopoietic prostaglandin D synthase; *GAPDH*= glyceraldehyde-3-phosphate dehydrogenase.

annotated using the KEGG database. Pearson correlation analysis was conducted using R language to explore the relationship between differential metabolites and clinical indicators.

2.9. Validation of oxylipin metabolomics results by RT-PCR

RT-PCR was used to determine the gene expression levels of phospholipase A2 group IVA (*PLA2G4*), elongase of very-long fatty acid 5 (*ELOVL5*), fatty acid desaturase 1 (*FADS1*), arachidonate 15-lipoxygenase (*ALOX15*), arachidonate 5-lipoxygenase (*ALOX5*), glutathione peroxidase 4 (*GPX4*), and hematopoietic prostaglandin D synthase (*HPGDS*) in the liver. The primers are shown in Table 2.

2.10. AA level in B. fragilis culture and the effects of AA on FLHS

The concentration of AA in the bacterial supernatant after 4, 8, 12 and 24 h of culture was detected by a commercial ELISA kit (Shanghai Jianglai Industrial Limited By Share Ltd., Shanghai, China).
Chicken LMH cells were cultured in DMEM (Thermo Fisher Scientific - CN, Shanghai, China) supplemented with 10% fetal bovine

serum (Beijing Aoqing Biotechnology Co., Ltd., Beijing, China) under humidified conditions of 37 °C and 5% CO_2. After monolayer LMH cells were grown to 85% confluence in six-well plates, they were exposed to 0.5 mmol/L free fatty acid (palmitic acid: oleic acid = 2:1) containing 0.5% bovine serum albumin to induce the cellular steatosis model and co-administered with AA (Solarbio, Beijing, China) at concentrations of 80 μmol/L for 24 h. These doses were screened by several cytotoxicity assays. The contents of TG and LDL-C in the cells were determined using commercial kits (Nanjing Jiancheng Bioengineering Institute, Jiangsu, China).

A total of 18 Jing Fen laying hens (1.56 ± 0.05 kg) were utilized in this animal experiment. The hens were randomly allocated into three groups (6 replicates per group and 1 hen per replicate). The control group received a basic diet (Contol), while the model group was fed the HELP diet. Additionally, the experimental group was provided with the HELP diet supplemented with 0.3% AA. The dose selection for AA administration was based on previous reports (Purba et al., 2021). The diets, feeding cycle, conditions, and environment for all hens remained consistent with those employed in the *B. fragilis* animal experiments. The experimental methods used in this section, such as liver pathology detection, blood biochemical detection, and gene expression detection, were consistent with those used in the *B. fragilis* experiment.

2.11. Statistical analyses

Statistical analysis and data visualization were performed using GraphPad Prism software (San Diego, CA, USA). The experimental unit for each variable's investigation was an individual laying hen. The clinical data such as blood lipids, body weight, etc., data on RT-PCR, differential oxylipin, and differential bacterial are presented as the mean ± SEM. The Shapiro−Wilk test was utilized to assess the normal distribution of the data, while the Levene test was employed to determine the homogeneity of variance. One-way ANOVA was used to test the significance between groups ($P < 0.05$), followed by Tukey's test for multiple group comparisons. The mathematical model used was as follows:

$$Y_{ij} = \mu + \alpha_i + \epsilon_{ij},$$

where Y_{ij} is the observed value of the dependent variable at the ith level for the jth observation. μ is the overall mean, α_i represents the effect at the ith level, and ϵ_{ij} is the random error, which follows an independent random variable distributed as n $(0, \sigma^2)$.

3. Results

3.1. B. fragilis ameliorated the clinical parameters of FLHS

In comparison to the Control group, laying hens fed a HELP diet exhibited a significant increase in body weight in the 7th week ($P = 0.006$). The laying hens of MBF group significantly reduced body weight at the 7th and 8th weeks compared to the HELP group ($P < 0.05$; Table 3). While the HBF and LBF intervention did not significantly alleviate body weight compared to the HELP group ($P > 0.05$; Table 3). There were no significant differences in average daily feed intake (ADFI) among all groups ($P = 0.873$). Correspondingly, all three doses of *B. fragilis* were able to decrease the liver weight and liver index compared to the HELP group ($P < 0.05$; Table 3). A gross anatomical examination of the liver in the HELP group revealed evident hepatic steatosis. Under the administration of *B. fragilis*, hepatic steatosis showed significant improvement, with the MBF group showing particularly remarkable improvement (Fig. 1). Histological staining with H&E and Oil Red O demonstrated that *B. fragilis* intervention ameliorated hepatic steatosis,

hepatocyte ballooning, and lipid deposition induced by the HELP diet (Fig. 1). *B. fragilis* intervention significantly improved liver damage, as evidenced by a notable reduction in the levels of AST and ALT in the serum ($P < 0.05$; Table 4). Prolonged consumption of the HELP diet led to elevated blood lipid levels in laying hens. Compared to the Control group, the HELP group showed a significant increase in TG, TC, and LDL-C levels, as well as a significant decrease in HDL-C levels, which were significantly reversed following *B. fragilis* supplementation ($P < 0.05$; Table 4). The improvement in laying hens TG, TC, and LDL-C levels among the three different doses of *B. fragilis* groups did not show significant differences. However, concerning the improvement in liver damage indicators, the MBF group exhibited a significant enhancement in both AST and ALT levels ($P < 0.05$). Considering body weight and liver pathology indicators, the MBF group demonstrated the most comprehensive improvement in FLHS. Therefore, the MBF group was selected for further experimental analysis.

3.2. B. fragilis improved lipid metabolism and inflammatory gene expression

To gain deeper insights into the ameliorative effects of *B. fragilis* on FLHS, key gene expression in FLHS pathology was assessed. The RT-PCR analysis results revealed that the HELP diet significantly elevated the gene expression of lipid synthesis-related genes *ACC*, *LXRα*, and *ASBT* ($P < 0.05$) compared to the Control group. Conversely, the administration of *B. fragilis* significantly reduced the expression levels of *FAS*, *LXRα*, and *ASBT* ($P < 0.05$; Fig. 2A). The HELP diet led to a reduction in the expression trends of the lipid oxidation genes *CPT-1*, *PPARα*, and *PPARγ* ($P > 0.05$), along with a significant increase in the gene expression of the inflammatory factors *TNF-α* and *IL-6* ($P < 0.05$). In comparison to the HELP group, the MBF group exhibited significant upregulation of the expression of lipid oxidation genes *CPT-1* and *PPARα* ($P < 0.05$), and notable downregulation of the expression of the inflammatory genes *TNF-α*, *IL-1β*, and *IL-6* ($P < 0.05$; Fig. 2B and C).

3.3. B. fragilis altered the gut microbiota structure and composition

The present study aimed to investigate the impact of *B. fragilis* on the structure of the intestinal microbiota in laying hens using 16S rRNA sequencing of cecal content samples. To determine the adequacy of sequencing depth and sample size, species dilution curves based on the Shannon index and species accumulation boxplots were employed. Fig. S2A demonstrates that the diversity index curve reached a plateau with increased sequencing data, indicating reasonable sequencing depth. Fig. S2B shows that species richness increased with larger sample sizes and then leveled off, indicating a sufficient sample size. Statistical results suggested that the HELP diet did not affect the α-diversity of the intestinal microbiota (Fig. 3A and B, Fig. S2C-E). The Dominance index, which indicated the evenness of the cecal microbiota tended to increase by *B. fragilis* administration compared to the HELP group ($P = 0.067$). Moreover, analysis of the Chao1, Simpson, and Shannon indexes indicated that *B. fragilis* had no impact on the α-diversity of the cecal microbiota (Fig. 3B, Fig. S2C-E). The effect of *B. fragilis* on the beta-diversity of the intestinal microbiota was similar. PCoA and nonmetric multidimensional scaling (NMDS) based on the Jaccard index revealed distinct clustering of the intestinal microbiota between the HELP group and the Control group, and also between the MBF and HELP groups (Fig. 3C, Fig. S2F). PCoA based on the Jaccard index solely considers species composition without taking into account species abundance. NMDS analysis based on unweighted UniFrac was difficult to use to clearly differentiate the cecal microbiota among the three

Table 3

Effects of *B. fragilis* on body weight, liver weight and ADFI of HELP-fed laying hens[1].

Item	Control	HELP	HBF	MBF	LBF	*P*-value
Body weight, kg						
0 week	1.54 ± 0.024	1.54 ± 0.039	1.58 ± 0.016	1.57 ± 0.018	1.55 ± 0.029	0.803
1 week	1.59 ± 0.026	1.62 ± 0.029	1.58 ± 0.022	1.55 ± 0.021	1.58 ± 0.023	0.378
2 week	1.63 ± 0.022	1.65 ± 0.027	1.61 ± 0.024	1.57 ± 0.021	1.60 ± 0.020	0.219
3 week	1.67 ± 0.024	1.70 ± 0.023	1.69 ± 0.028	1.64 ± 0.022	1.66 ± 0.016	0.412
4 week	1.63 ± 0.023	1.59 ± 0.022	1.64 ± 0.029	1.67 ± 0.023	1.64 ± 0.029	0.268
5 week	1.65 ± 0.027	1.72 ± 0.025	1.69 ± 0.035	1.61 ± 0.023	1.66 ± 0.021	0.061
6 week	1.66 ± 0.031	1.73 ± 0.027	1.70 ± 0.035	1.62 ± 0.024	1.68 ± 0.019	0.072
7 week	1.65 ± 0.025[b]	1.77 ± 0.022[a]	1.72 ± 0.036[ab]	1.64 ± 0.024[b]	1.71 ± 0.021[ab]	0.006
8 week	1.65 ± 0.028[ab]	1.76 ± 0.024[a]	1.69 ± 0.040[a]	1.63 ± 0.023[b]	1.67 ± 0.022[ab]	0.022
Liver weight, g	31.92 ± 0.417[b]	37.67 ± 1.430[a]	31.35 ± 0.891[b]	31.14 ± 0.666[b]	31.69 ± 0.654[b]	<0.001
Liver index, %	1.95 ± 0.024[b]	2.16 ± 0.084[a]	1.85 ± 0.035[b]	1.97 ± 0.036[b]	1.85 ± 0.040[b]	<0.001
ADFI, g	103.60 ± 2.826	107.10 ± 2.456	105.80 ± 3.031	104.60 ± 2.662	104.10 ± 1.930	0.873

ADFI = average daily feed intake; HELP = high-energy and low-protein.

[a,b]Mean values within a row with different superscript letters indicate significant difference (*P* < 0.05). Values are means ± SEM, *n* = 8.

[1] Control = control group, hens fed with standard diet; HELP = model group, hens fed with high-energy low-protein diet; HBF, MBF, and LBF = experimental groups, hens fed with high-energy low-protein diet and administrated with 10^{10}, 10^{9}, and 10^{8} CFU *B. fragilis*, respectively.
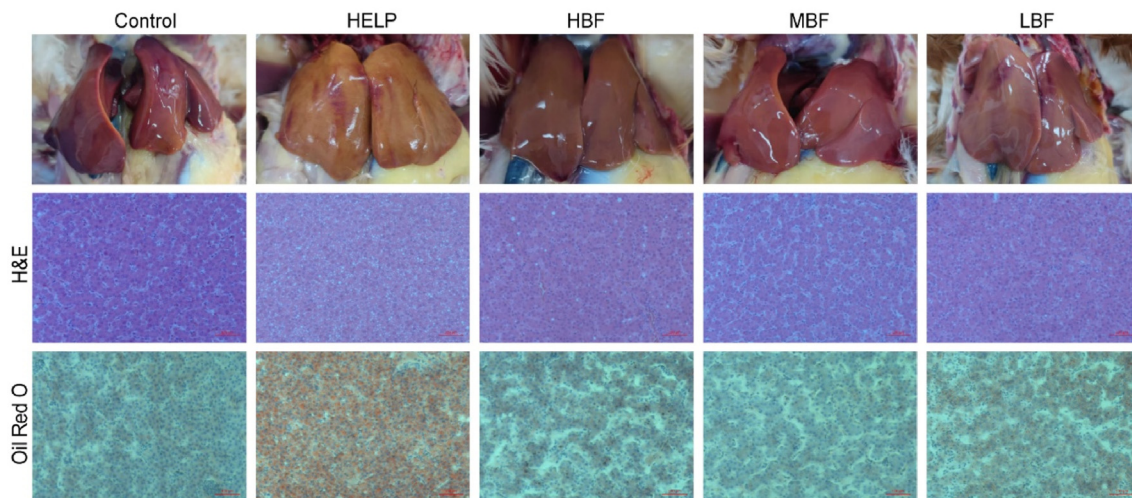

Fig. 1. *B. fragilis* improved hepatic lipid deposition induced by the high-energy and low-protein (HELP) diet. Liver gross morphology, hematoxylin and eosin (H&E) staining, and Oil Red O staining. The scale bar on the figure is 100 μm. Control = control group, hens fed with standard diet; HELP = model group, hens fed with high-energy low-protein diet; HBF, MBF, and LBF = experimental groups, hens fed with high-energy low-protein diet and administrated with 10^{10}, 10^{9}, and 10^{8} CFU *B. fragilis*, respectively.

Table 4

B. fragilis improved blood lipids and liver function in serum [1].

Item	Control	HELP	HBF	MBF	LBF	*P*-value
TG, mmol/L	19.14 ± 0.857[b]	27.17 ± 1.260[a]	20.87 ± 1.194[b]	20.23 ± 1.301[b]	20.81 ± 1.161[b]	<0.001
TC, mmol/L	2.75 ± 0.095[b]	4.03 ± 0.137[a]	3.02 ± 0.172[b]	3.32 ± 0.081[b]	3.33 ± 0.180[b]	<0.001
LDL-C, mmol/L	0.76 ± 0.047[b]	1.10 ± 0.046[a]	0.76 ± 0.048[b]	0.81 ± 0.057[b]	0.85 ± 0.064[b]	<0.001
HDL-C, mmol/L	0.88 ± 0.051[a]	0.68 ± 0.041[bc]	0.77 ± 0.057[ab]	0.71 ± 0.053[ab]	0.59 ± 0.041[c]	0.003
AST, U/L	166.60 ± 3.760[b]	191.00 ± 7.273[a]	182.30 ± 7.319[ab]	165.90 ± 5.535[b]	178.40 ± 3.903[ab]	0.021
ALT, U/L	5.34 ± 0.328[b]	6.64 ± 0.358[a]	5.96 ± 0.336[ab]	4.70 ± 0.261[b]	4.31 ± 0.320[b]	<0.001

TG = triglyceride; TC = total cholesterol; HDL-C = high density lipoprotein cholesterol; LDL-C = low density lipoprotein cholesterol; AST = aspartate aminotransferase; ALT = alanine aminotransferase.

[a-c]Mean values within a row with different superscript letters indicate significant difference (*P* < 0.05). Values are means ± SEM, *n* = 8.

[1] Control = control group, hens fed with standard diet; HELP = model group, hens fed with high-energy low-protein diet; HBF, MBF, and LBF = experimental groups, hens fed with high-energy low-protein diet and administrated with 10^{10}, 10^{9}, and 10^{8} CFU *B. fragilis*, respectively.

groups (Fig. S2G). To assess the appropriateness of the grouping, an analysis of similarities (ANOSIM) based on the Bray—Curtis distance was conducted to analyze the differences within and between groups. Table S1 shows that the *R*-values for all pairwise comparisons among the three groups exceeded 0, indicating greater differences between the groups than within. In summary, *B. fragilis* had an impact on the cecal microbiota structure to some extent, but the impact was not significant.

Furthermore, the composition of the cecal microbiota was analyzed. At the phylum level, Bacteroidota and Firmicutes were the predominant phyla in the cecum, accounting for approximately 90% of the total, followed by Euryarchaeota (Fig. 3E). The HELP diet led to a decrease in Bacteroidota and an increase in Firmicutes, while the administration of *B. fragilis* reversed these effects (Fig. 3E). Firmicutes and Bacteroidota were closely associated with host lipid metabolism, and the ratio of Firmicutes to Bacteroidota
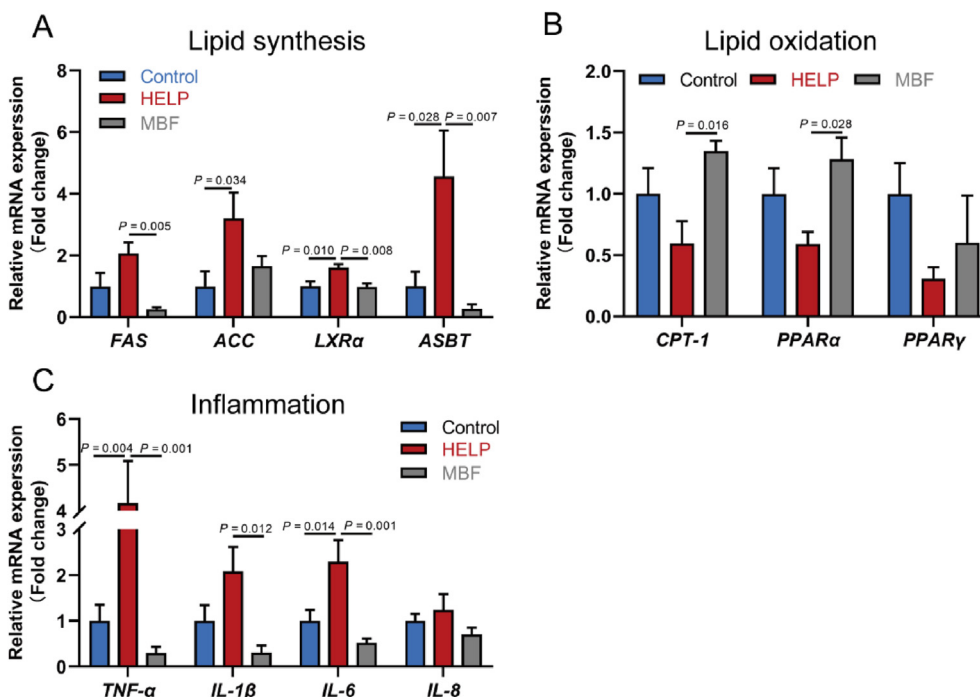
Fig. 2. *B. fragilis* improved the expression of lipid metabolism and inflammatory factor-related genes. (A) Relative mRNA expression of lipid synthesis-related genes. (B) Relative mRNA expression of lipid oxidation-related genes. (C) Relative mRNA expression of inflammatory factor-related genes. Control = control group, hens fed with standard diet; HELP = model group, hens fed with high-energy low-protein diet; MBF = experimental group, hens fed with high-energy low-protein diet and administrated with 10^9 CFU *B. fragilis*; *FAS* = fatty acid synthase; *ACC* = acetyl-CoA carboxylase; *LXRα* = liver X receptor α; *ASBT* = apical sodium-dependent bile acid transporter; *PPAR* = peroxisome proliferator activated receptor; *CPT-1* = carnitine palmitoyl transferase-1; *TNF-α* = tumor necrosis factor-α; *IL* = interleukin. Values are presented as means ± SEM ($n = 6$). When $P < 0.05$, the difference between the two groups is significant.

(F/B ratio) was positively correlated with NAFLD. The *B. fragilis* intervention reduced the F/B ratio, but the reduction was not significant (Fig. 3G). Additionally, the *B. fragilis* intervention significantly decreased the relative abundance of Proteobacteria ($P = 0.040$; Fig. 3H). At the genus level, the bacterial composition of the MBF group was more similar to the Control group (Fig. 3F). The HELP diet altered the relative abundance of bacterial species, with a decrease in *Monoglobus* and *Clostridiales DTU089* ($P < 0.05$), and an increase in *Succinatimonas* and *Faecalicoccus* ($P < 0.05$), while the MBF group exhibited the opposite trend (Fig. 3J). As presented in Fig. 3F, *Bacteroides* exhibited a significantly higher relative abundance compared to other genera, indicating its dominant position in the intestinal microbiota. Additionally, LEfSe analysis revealed that Bacteroidota and *Bacteroides* were significantly enriched in the MBF group and served as indicative bacteria (Fig. 3I). Metastat analysis also confirmed the contribution of *Bacteroides* ($P = 0.007$, Fig. 3K). In conclusion, the addition of *B. fragilis* reversed the changes in the intestinal microbiota caused by the HELP diet, enriching *Bacteroides*, which positively affected liver lipid metabolism.

3.4. Changes in gut microbiota by B. fragilis related to FLHS

In the aforementioned study, we identified five distinct bacterial species exhibiting differential abundance. By conducting a Spearman correlation analysis between these differential bacteria and disease-associated markers, we delved into the potential influence of these bacteria on the disease state. Our analysis revealed significant negative correlations between *Bacteroides* and *Clostridiales DTU089* with TG, TC, and LDL-C levels ($P < 0.05$), suggesting a potential lipid-modulating effect by these bacterial taxa. Notably, *Bacteroides* exhibited a positive correlation with AST ($P = 0.014$), indicating a potential dual role involving lipid metabolism

improvement and potential liver function implications. Conversely, *Faecalicoccus* demonstrated significant positive correlations with TG, TC, and LDL-C levels ($P < 0.05$), implying a potential risk factor for the occurrence of FLHS (Fig. 4A). Further insights emerged from our enrichment analysis of the gut microbiota using KEGG pathways, revealing the noteworthy downregulation of three Level 3 metabolic pathways (Fig. 4B). These pathways encompass retrograde endocannabinoid signaling, NAFLD, and regulation of lipolysis in adipocytes, pointing to substantial alterations in lipid-related metabolic routes (Fig. 4C–E).

3.5. B. fragilis ameliorated disrupted oxylipin metabolism in FLHS hens

To investigate the impact of *B. fragilis* on oxylipin metabolism in the liver of laying hens, targeted lipidomics focusing on oxylipin was utilized to analyze the composition and content of oxylipins among the three groups. As shown in Fig. S3A, the QC samples exhibited a high degree of total ion flow overlap, indicating the instrument's stability. Fig. S3B demonstrates that the Pearson correlation coefficient among QC samples approaches 1, signifying high data quality. The distribution of coefficient of variation (CV) values among QC samples, as depicted in Fig. S3C, revealed that substances with CV values less than 0.2 accounted for over 80%, underscoring the experiment's remarkable stability. Furthermore, in the PCA score plot, all QC samples clustered closely, suggesting a consistent instrument performance (Fig. S3D). While PCA did not strongly discriminate between the three groups, OPLS-DA, which was more sensitive to less correlated variables, was subsequently employed. The OPLS-DA results exhibited a clear separation between the Control group and the HELP group, indicating disrupted oxylipin metabolism in FLHS chickens (Fig. 5A). Additionally, there was a notable separation between the MBF group and the HELP
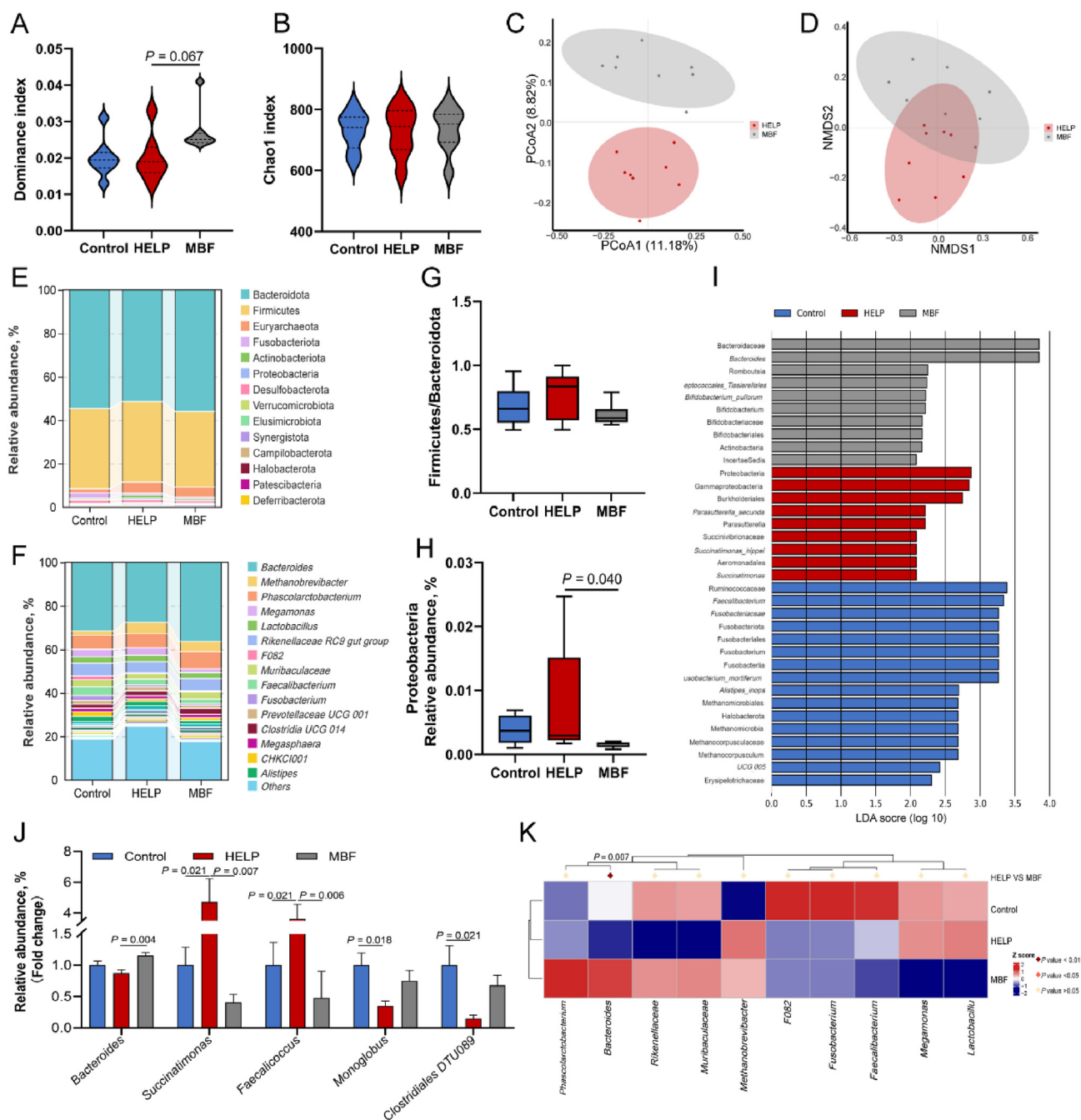
Fig. 3. *B. fragilis* improved the gut microbial structure and taxonomic composition induced by high-energy and low-protein. (A-B) α-Diversity analysis. (C) Principal coordinate analysis (PCoA) of the HELP and MBF groups. (D) Nonmetric multidimensional scaling (NMDS) analysis of the HELP and MBF groups. (E) Relative abundance of gut microbial species composition at the phylum level. (F) Relative abundance of gut microbial species composition at the genus level. (G) Proportions of Firmicutes and Bacteroidetes. (H) Relative abundance of Proteobacteria. (I) Linear discriminant analysis effect size (linear discriminant analysis score >2). (J) Differential genus-level analysis. (K) Metastat analysis for identifying intergroup differential genera. Control = control group, hens fed with standard diet; HELP = model group, hens fed with high-energy low-protein diet; MBF = experimental group, hens fed with high-energy low-protein diet and administrated with 10^9 CFU *B. fragilis*. Values are presented as means ± SEM ($n = 8$). When $P < 0.05$, the difference between the two groups is significant.

group, suggesting an improvement in oxylipin metabolism following intervention with *B. fragilis* (Fig. 5B).

The intervention of the HELP diet and *B. fragilis* resulted in alterations in various polyunsaturated fatty acid metabolites. As illustrated in Fig. 5C, compared to the Control group, the HELP diet resulted in the upregulation of three substances and the downregulation of four substances. In comparison to the HELP group, the MBF group exhibited upregulation of four substances and downregulation of five substances (Fig. 5D). In total, twelve differential

metabolites were detected, comprising six metabolites related to the AA metabolic pathway, two related to the linoleic acid (LA) metabolic pathway, and two related to the eicosapentaenoic acid (EPA) metabolic pathway (Table 5).

As shown in Fig. 5E, compared to the HELP group, *B. fragilis* intervention led to an 18.72% increase in AA content, reaching 1782 nmol/g, significantly improving the decrease caused by the HELP diet ($P = 0.008$). Moreover, after *B. fragilis* intervention, the levels of the metabolic pathway products 15-keto-prostaglandin E2
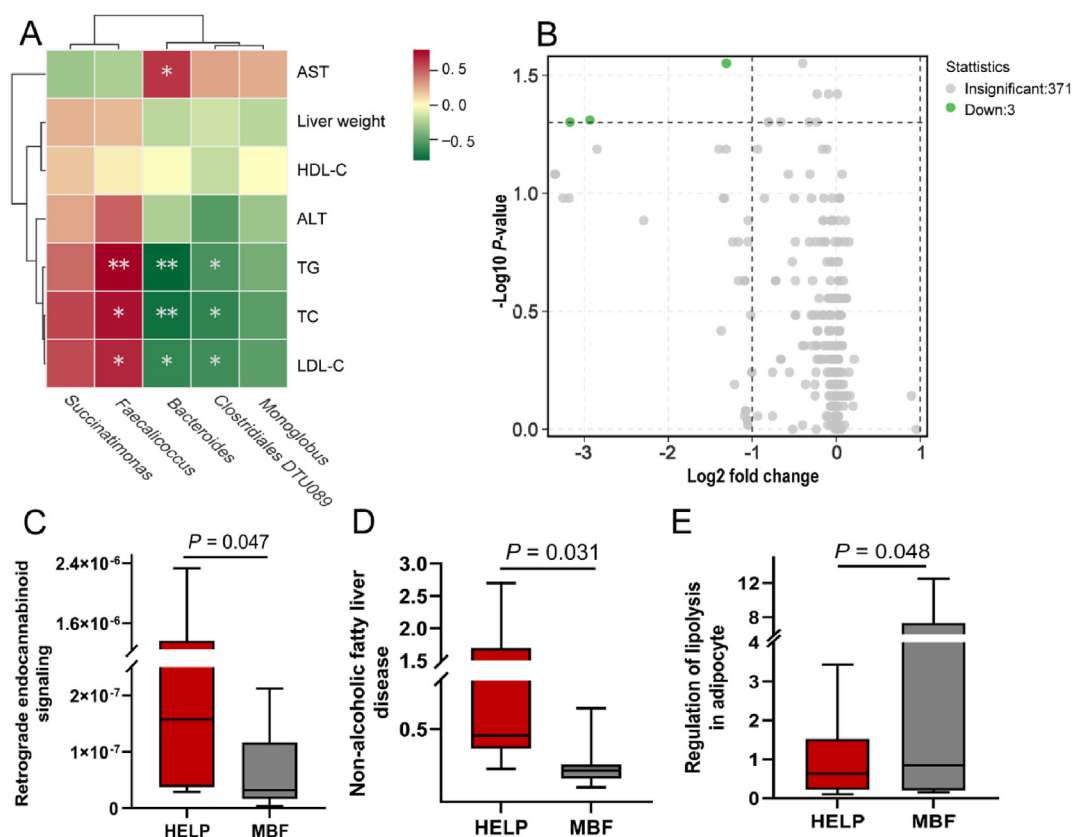
Fig. 4. Analysis of differential microbes in conjunction with disease-related indices and Kyoto encyclopedia of genes and genomes pathway enrichment. (A) Correlation analysis between differential microbes and disease indices. *$P < 0.05$ and **$P < 0.01$. (B) Differential pathway volcano plot. (C-E) Enriched differential metabolic pathways. HELP = model group, hens fed with high-energy low-protein diet; MBF = experimental group, hens fed with high-energy low-protein diet and administrated with 10^9 CFU *B. fragilis*; TG = triglyceride; TC = total cholesterol; HDL-C = high density lipoprotein cholesterol; LDL-C = low density lipoprotein cholesterol; AST = aspartate aminotransferase; ALT = alanine aminotransferase. Values are presented as means ± SEM ($n = 8$). When $P < 0.05$, the difference between the two groups is significant.

(15-keto-PGE$_2$), 15-oxoeicosatetraenoic acid (15-oxoETE), and 12-oxoeicosatetraenoic acid (12-oxoETE) were significantly down-regulated ($P < 0.05$), while the contents of PGD$_2$ were upregulated ($P = 0.070$), all exhibiting similar trends to the Control group (Table 5). In the livers of laying hens fed *B. fragilis*, LA levels significantly increased ($P = 0.001$), showing 18% growth compared to the Control group and 16.67% growth compared to the HELP group ($P = 0.001$; Fig. 5E). The HELP diet resulted in a decrease in the LA metabolite 13-oxo-9Z,11E-octadecadienoic acid (13-oxoODE) ($P = 0.124$) and an increase in PGK$_1$ ($P = 0.346$) and 13(S)-hydroperoxy-9Z, 11E-octadecadienoic acid (13(S)-HpODE) ($P = 0.079$), while *B. fragilis* intervention restored these levels to those of the Control group, showing improvement (Table 5). Similarly, the HELP diet led to an increase in the EPA metabolite 11-hydroxy-EPA (11-HEPE) ($P = 0.393$), which was improved by *B. fragilis* intervention. Compared to the Control group, the levels of 5S-hydroxy-6E,8Z,11Z-eicosatrienoic acid (5-HETrE) were significantly reduced by 66.41% and 71% in the HELP group and MBF group, respectively ($P < 0.001$). The intervention of *B. fragilis* did not lead to a further decrease in its content (Table 5). Through the analysis of different metabolites, it was found that the addition of *B. fragilis* mainly improved the AA metabolic pathway.

Pearson correlation analysis was performed to explore the associations among differential metabolites and blood lipids. As shown in Fig. 5F, there was a strong positive correlation among 12-oxoETE, 15-oxoETE, 15-keto-PGE$_2$, and 13(S)-HpODE ($P < 0.01$). These metabolites are known for their proinflammatory activities and showed similar changes in the oxylipin metabolism pathway. Notably, AA, a metabolite of LA, exhibited negative correlations

with the mentioned pro-inflammatory substances, particularly significant negative correlations with 13(S)-HpODE and 12-oxoETE ($P < 0.05$). Moreover, in the LA metabolic pathway, LA is metabolized to γ-LA, and then subsequently to dihomo-γ-linolenic acid (D-γ-LA) and AA. Comparing the HELP and Control groups, AA was downregulated, but after intervention with *B. fragilis*, their levels were restored to levels similar to those of the Control group ($P = 0.008$; Fig. 5E). The correlation analysis in Fig. 5F supports this observation, showing that AA has significant positive correlations with LA and D-γ-LA ($P < 0.05$). To investigate the impact of differential *B. fragilis* on FLHS, we analyzed the Pearson correlation between metabolites and clinical indicators related to FLHS. In Fig. 5G, AA demonstrates significant negative correlations with TG, TC, LDL-C, and liver weight ($P < 0.05$). Similarly, D-γ-LA showed significant negative correlations with TG, TC, and LDL-C ($P < 0.05$). There was a significant negative correlation observed between LA and the liver function marker ALT ($P = 0.043$). Additionally, PGD$_2$ and 5-HETrE exhibited a significant negative correlation with TC and liver weight ($P < 0.05$).

3.6. B. fragilis modulated the oxylipin metabolism pathway and key enzymes

B. fragilis induced alterations in oxylipin metabolism, which was further elucidated by comparing differential metabolites against the KEGG database. To validate the impact of *B. fragilis* on the oxylipin metabolic pathway, RT-PCR was conducted to observe the transcription levels of relevant genes. In comparison to the Control group, the HELP diet significantly downregulated the expression
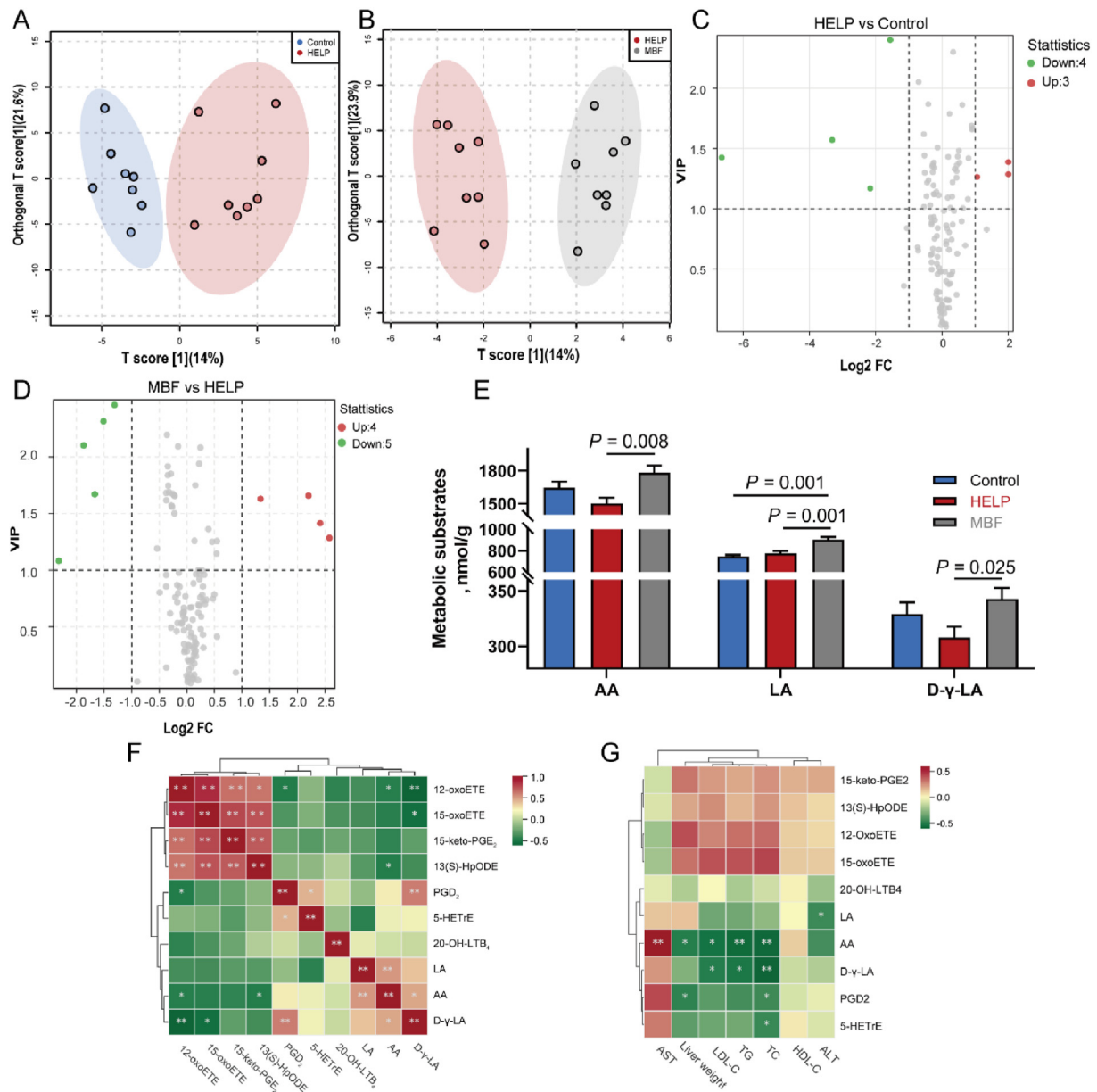
Fig. 5. *B. fragilis* improved oxylipin metabolism disruption induced by the high-energy and low-protein diet. (A-B) orthogonal partial least squares discriminant analysis (OPLS-DA) between the two groups. (C-D) Volcano plot of differential metabolites. (E) Changes in the content of oxylipin metabolism pathway substrates. (F) Pearson correlation analysis between metabolites. *$P < 0.05$ and **$P < 0.01$. (G) Pearson correlation analysis between metabolites and clinical indicators of the disease. *$P < 0.05$ and **$P < 0.01$. Control = control group, hens fed with standard diet; HELP = model group, hens fed with high-energy low-protein diet; MBF = experimental group, hens fed with high-energy low-protein diet and administrated with 10^9 CFU *B. fragilis*; VIP = variable importance in the projection; FC = fold change; AA = arachidonic acid; LA = linoleic acid; D-γ-LA = dihomo-γ-linolenic acid; 15-oxoETE = 15-oxoeicosatetraenoic acid; 12-oxoETE = 12-oxoeicosatetraenoic acid; 20-OH-LTB$_4$ = 20-OH-leukotriene B$_4$; 13(S)-HpODE = 13(S)-hydroperoxy-9Z,11E-octadeca-dienoic acid; 15-keto-PGE$_2$ = 15-keto-prostaglandin E$_2$; PGD$_2$ = prostaglandin D$_2$; 5-HETrE = 5S-hydroxy-6E,8Z,11Z-eicosatrienoic acid; TG = triglyceride; TC = total cholesterol; HDL-C = high density lipoprotein cholesterol; LDL-C = low density lipoprotein cholesterol; AST = aspartate aminotransferase; ALT = alanine aminotransferase. Values are presented as means ± SEM ($n = 8$). When $P < 0.05$, the difference between the two groups is significant.

levels of *PLA2G4*, *ELOVL5*, and *GPX4*, by approximately 0.39-, 0.46-, and 0.5-fold, respectively ($P < 0.05$; Fig. 6). *B. fragilis* intervention significantly elevated the expression of *GPX4* and enhanced the expression trends of *PLA2G4* and *ELOVL5* ($P < 0.05$). Specifically, in contrast to the HELP group, *GPX4* expression increased by 1.82-fold, while *PLA2G4* and *ELOVL5* expression increased by 2.11- and 1.8-fold, respectively ($P < 0.05$; Fig. 6). The gene expression levels of *ALOX15* and *ALOX5* in the HELP group are notably elevated by 2.6-and 4.23-fold, respectively, compared to the Control group ($P < 0.05$). However, *B. fragilis* intervention reduced these levels to 0.5- and 0.8-fold, respectively ($P < 0.05$; Fig. 6). Additionally, while

the gene expression levels of *FADS1* and *HPGDS* did not exhibit significant changes among the three groups, both showed decreasing trends after the HELP diet intervention, which was nearly restored to the Control group levels following *B. fragilis* intervention ($P > 0.05$; Fig. 6).

3.7. Integration analysis of oxylipin metabolomics and gut microbiota

To establish the potential associations between distinct bacterial taxa and identified differential lipid metabolites, Spearman

Table 5
B. fragilis altered oxylipin metabolites (nmol/mg) of the liver in HELP-fed laying hens[1].

Item	Class	Control	HELP	MBF	P-value	Pathway
15-OxoETE	AA	1.29 ± 0.328^b	2.39 ± 0.401^a	0.66 ± 0.229^b	0.004	AA
12-OxoETE	AA	6.90 ± 2.227^{ab}	12.01 ± 1.286^a	4.22 ± 1.837^b	0.022	AA
15-Keto-PGE$_2$	AA	4.49 ± 1.406^a	8.43 ± 1.263^a	3.40 ± 0.387^b	0.011	AA
PGD$_2$	AA	4.69 ± 1.635	0.47 ± 0.471	2.51 ± 1.231	0.070	AA
20-OH-LTB$_4$	AA	0.98 ± 0.346	0.58 ± 0.288	1.47 ± 0.337	0.176	AA
LXB$_4$	AA	4.57 ± 2.246	ND	1.11 ± 1.113	0.089	AA
13(S)-HpODE	LA	1.68 ± 0.593	3.50 ± 0.938	1.10 ± 0.637	0.079	LA
13-OxoODE	LA	ND	1.14 ± 0.751	ND	0.124	LA
PGK$_1$	D-γ-LA	9.79 ± 9.794	ND	20.35 ± 13.490	0.346	–
11-HEPE	EPA	1.03 ± 0.539	0.23 ± 0.228	1.05 ± 0.578	0.393	EPA
LXA$_5$	EPA	ND	2.23 ± 1.240	ND	0.276	EPA
5-HETrE	–	13.07 ± 1.909^a	$4.43 \pm 0.424^{b,c}$	3.84 ± 0.234^c	<0.001	–

HELP = high-energy and low-protein; ND = not detected; AA = arachidonic acid; LA = linoleic acid; EPA = eicosapentaenoic acid; D-γ-LA = dihomo-γ-linolenic acid; 15-oxoETE = 15-oxoeicosatetraenoic acid; 12-oxoETE = 12-oxoeicosatetraenoic acid; 15-keto-PGE$_2$= 15-keto-prostaglandin E$_2$; PGD$_2$ = prostaglandin D$_2$; 20-OH-LTB$_4$= 20-OH-leukotriene B$_4$; LXB$_4$ = 5S,14R,15S-trihydroxy-6E, 8Z,10E,12E-eicosatetraenoic acid; 13(S)-HpODE = 13(S)-hydroperoxy-9Z, 11E-octadecadienoic acid; 13-oxoODE = 13-oxo-9Z, 11E-octadecadienoic acid; PGK$_1$ = prostaglandin K$_1$; 11-HEPE = 11-hydroxy-EPA; LXA$_5$ = 5S,6R,15S-trihydroxy-7E, 9E,11Z,13E,17Z-eicosapentaenoic; 5-HETrE = 5S-hydroxy-6E, 8Z,11Z-eicosatrienoic acid.
[a-c]Mean values within a row with different superscript letters indicate significant difference ($P < 0.05$). Values are means $\pm$ SEM, $n = 8$.
[1] Control = control group, hens fed with standard diet; HELP = model group, hens fed with high-energy low-protein diet; MBF = experimental group, hens fed with high-energy low-protein diet and administrated with 10^9 CFU *B. fragilis*.
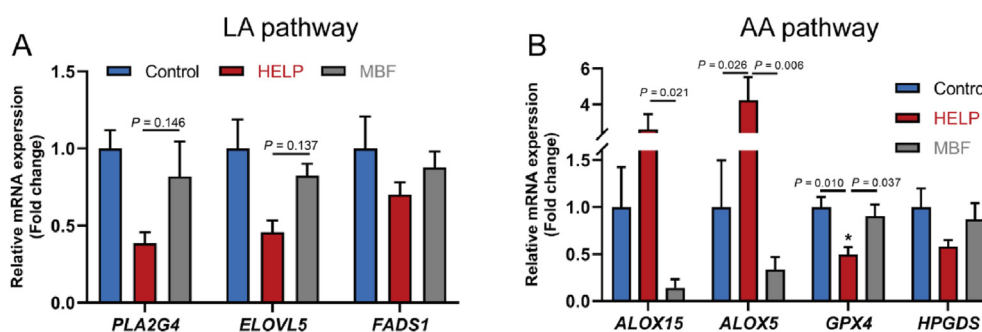

Fig. 6. Impact of *B. fragilis* on the hepatic oxylipin metabolism pathway. (A) Relative mRNA expression of linoleic acid (LA) pathway. (B) Relative mRNA expression of arachidonic acid (AA) pathway. Control = control group, hens fed with standard diet; HELP = model group, hens fed with high-energy low-protein diet; MBF = experimental group, hens fed with high-energy low-protein diet and administrated with 10^9 CFU *B. fragilis*. PLA2G4 = phospholipase A2 group IVA; ELOVL5 = elongase of very-long fatty acid 5; FADS1 = fatty acid desaturase 1; ALOX15 = arachidonate 15-lipoxygenase; ALOX5 = arachidonate 5-lipoxygenase; GPX4 = glutathione peroxidase 4; HPGDS = hematopoietic prostaglandin D synthase. Values are presented as means $\pm$ SEM ($n = 6$). When $P < 0.05$, the difference between the two groups is significant.

correlation analysis was performed. As depicted in Fig. 7A, *Succinatimonas* exhibited significant positive correlations with proinflammatory compounds, including 15-oxoETE, 15-keto-PGE$_2$, 12-oxoETE, and 13(S)-HpODE ($P < 0.05$), while displaying a significant negative correlation with LA ($P = 0.026$). Notably, *Monoglobus* demonstrated a significant negative correlation with 15-keto-PGE$_2$ ($P = 0.031$). Furthermore, *Bacteroides* displayed significant positive correlations with AA and LA ($P < 0.05$; Fig. 7A). Given *Bacteroides*' status as a dominant species in the cecum and AA's role as both a substrate in the AA metabolic pathway and a prominent constituent, their interaction was crucial in maintaining stability. Consequently, a Pearson correlation analysis was employed to investigate their relationship. The results revealed a linear relationship, indicating that an increase in AA concentration corresponded to an increase in *Bacteroides* relative abundance ($P = 0.007$; Fig. 7B). This suggests that *Bacteroides* might modulate FLHS through AA regulation. To substantiate this, ELISA was utilized to assess the AA content in the *B. fragilis* culture supernatant. The results showed that *B. fragilis* secretes AA, with its concentration gradually increasing over time and stabilizing after 12 h (Fig. 7C).

3.8. Metabolites of B. fragilis alleviate FLHS in laying hens

To validate the direct effect of AA on the liver, LMH cell experiments were conducted to assess the cellular impact of AA. The main focus was on lipid content within LMH cells. The results revealed that the addition of 80 μmol/L AA to the cell culture medium significantly decreased the levels of TG and LDL-C ($P < 0.05$; Table 6). In the animal experiment, starting from the seventh week, the body weight of laying hens fed the HELP diet increased significantly ($P = 0.007$), and by the eighth week, the AA group exhibited significantly lower body weight than the Model group ($P = 0.005$), indicating that supplementation with AA improved weight (Table 7). There was no significant difference in ADFI between the groups ($P = 0.432$; Table 7). The addition of AA to the feed improved hepatic steatosis and liver damage. Compared to the Model group, the AA group showed significant reductions in liver weight ($P < 0.001$; Table 7). H&E staining and Oil Red O staining revealed fewer lipid vacuoles and lipid deposits in the AA group (Fig. 8). Moreover, AST and ALT levels were significantly reduced in the AA group ($P < 0.05$), indicating an improvement in liver injury (Table 8). Serum lipid analysis demonstrated that AA effectively ameliorated the increases in TG, TC, and LDL-C induced by the HELP diet ($P < 0.05$), and significantly raised HDL-C level ($P = 0.039$; Table 8). Collectively, the combination of in vivo and in vitro assessments confirmed that AA had the potential to ameliorate hepatic steatosis in laying hens and directly improve liver cell conditions.

To elucidate the mechanisms underlying the alleviating effects of AA on FLHS, we employed RT-PCR analysis to investigate changes in genes related to lipid metabolism and oxylipin pathways. The
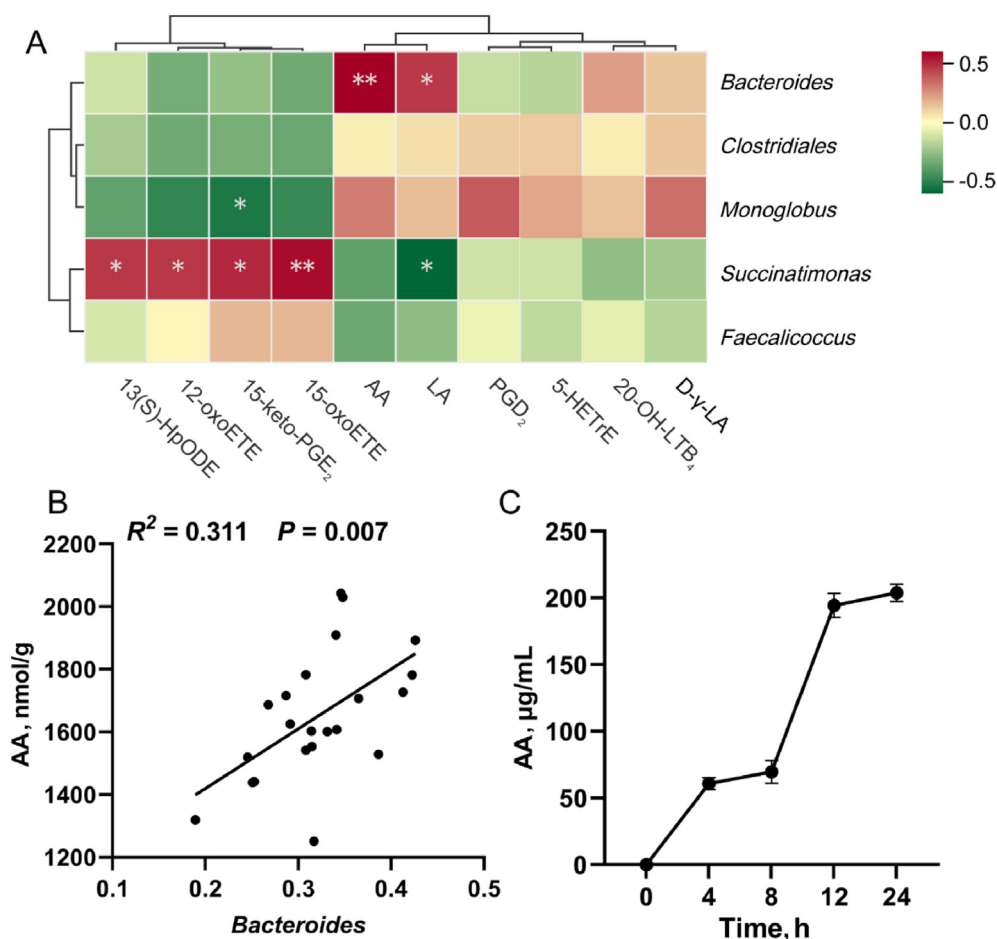
Fig. 7. Combined analysis of intestinal flora and oxylipin metabolomics. (A) Spearman correlation analysis between differential metabolites and differential bacteria. *$P < 0.05$ and **$P < 0.01$. $n = 8$. (B) Pearson correlation analysis between arachidonic acid (AA) and *Bacteroides*. $n = 8$. (C) AA content in the supernatant of *B. fragilis* medium, values are presented as means ± SEM ($n = 4$). D-γ-LA = dihomo-γ-linolenic acid; 15-oxoETE = 15-oxoeicosatetraenoic acid; 12-oxoETE = 12-oxoeicosatetraenoic acid; 20-OH-LTB$_4$ = 20-OH-leukotriene B$_4$; 13(S)-HpODE = 13(S)-hydroperoxy-9Z,11E-octadecadienoic acid; 15-keto-PGE$_2$ = 15-keto-prostaglandin E$_2$; PGD$_2$ = prostaglandin D$_2$; 5-HETrE = 5S-hydroxy-6E,8Z,11Z-eicosatrienoic acid. When $P < 0.05$, the difference between the two groups is significant.

Table 6
AA reduced lipid accumulation induced by fatty acids in LMH cells (mmol/g prot)[1].

Item	Con	Model	AA	P-value
TG	0.07 ± 0.016^b	0.24 ± 0.024^a	0.14 ± 0.020^b	0.002
TC	0.08 ± 0.012	0.10 ± 0.008	0.09 ± 0.016	0.635
LDL-C	0.04 ± 0.007^b	0.08 ± 0.012^a	0.04 ± 0.006^b	0.014
HDL-C	0.04 ± 0.004^a	0.02 ± 0.002^b	0.03 ± 0.006^a	0.045

AA = arachidonic acid; TG = triglyceride; TC = total cholesterol; HDL-C = high density lipoprotein cholesterol; LDL-C = low density lipoprotein cholesterol.
[a,b] Mean values within a row with different superscript letters indicate significant difference ($P < 0.05$). Values are means ± SEM, $n = 3$.
[1] Con = control group, LMH, cells treated with only the culture medium; Model = model group, LMH, cells induced with oleic acid and palmitic acid for lipid degeneration; AA = experimental groups, Model group with the addition of 80 μmol/L AA.

HELP diet upregulated the expression of lipid synthesis-related genes, including *FAS*, *ACC*, *LXRα*, and *ASBT* ($P < 0.05$). Conversely, AA significantly inhibited the expression of *FAS*, *LXRα*, and *ASBT* ($P < 0.05$), with no observed impact on *ACC* expression (Fig. 9A). In terms of lipid oxidation gene expression, AA reversed the down-regulation of *CPT-1* and *PPARα* gene expression caused by the HELP diet ($P < 0.05$), thereby enhancing the expression of fatty acid oxidation genes (Fig. 9B). The amelioration of inflammation-related gene expression by AA is noteworthy, as the increased gene expression of *TNF-α*, *IL-1β*, *IL-6*, and *IL-8* observed in the Model group was significantly attenuated by AA ($P < 0.05$; Fig. 9C). To verify whether the effects of AA on improving oxylipin pathway-related genes were similar to those of *B. fragilis*, we assessed the expression of relevant genes. The results demonstrated that within the LA metabolic pathway, AA remarkably ameliorated the reduced expression of the *PLA2G4* gene caused by the HELP diet ($P = 0.081$). While the effects on the expression of the *ELOVL5* and *FADS1* genes were not significant, the trends remained consistent with the impact of *B. fragilis* (Fig. 9D). Within the AA metabolic pathway, compared to the Control group, the Model group significantly increased the expression of *ALOX5* ($P = 0.041$), and *ALOX15* also exhibited an increasing trend ($P = 0.070$). The addition of AA significantly reduced the expression of both *ALOX5* and *ALOX15* ($P < 0.05$). The HELP diet led to a notable decrease in *GPX4* gene expression ($P = 0.001$), and *HPGDS* gene expression displayed a decreasing trend ($P = 0.064$). Remarkably, AA significantly upregulated *GPX4* expression ($P = 0.004$), while the increase in *HPGDS* gene expression was not significant (Fig. 9E). These results indicated that AA's ameliorative effects within the AA metabolic pathway exhibited similarities to those of *B. fragilis*.

Table 7
AA improved body weight and liver weight gain in FLHS-affected laying hens[1].

Item	Con	Model	AA	P-value
Body weight, kg				
0 week	1.55 ± 0.021	1.57 ± 0.022	1.55 ± 0.025	0.856
1 week	1.61 ± 0.026	1.63 ± 0.024	1.58 ± 0.029	0.534
2 week	1.64 ± 0.021	1.65 ± 0.028	1.60 ± 0.028	0.326
3 week	1.65 ± 0.024	1.68 ± 0.019	1.62 ± 0.014	0.125
4 week	1.64 ± 0.027	1.68 ± 0.022	1.63 ± 0.025	0.375
5 week	1.65 ± 0.026	1.72 ± 0.027	1.69 ± 0.030	0.207
6 week	1.66 ± 0.027	1.75 ± 0.029	1.70 ± 0.025	0.084
7 week	1.65 ± 0.030[b]	1.78 ± 0.022[a]	1.70 ± 0.021[ab]	0.007
8 week	1.66 ± 0.026[b]	1.79 ± 0.017[a]	1.69 ± 0.021[b]	0.005
Liver weight, g	32.18 ± 0.571[b]	37.27 ± 1.636[a]	33.72 ± 0.808[b]	<0.001
Liver index, %	1.91 ± 0.015[b]	2.18 ± 0.054[a]	1.99 ± 0.044[b]	<0.001
ADFI, g	105.30 ± 1.127	106.60 ± 1.138	103.90 ± 1.893	0.432

AA = arachidonic acid; FLHS = fatty liver hemorrhagic syndrome; ADFI = average daily feed intake.
[a,b] Mean values within a row with different superscript letters indicate significant difference ($P < 0.05$). Values are means ± SEM, n= 8.
[1] Con = control group, hens fed with standard diet; Model = model group, hens fed with high-energy low-protein diet; AA = experimental groups, hens fed with high-energy low-protein diet with 0.3 % AA.

4. Discussion

Gut microbiota dysbiosis can result in compromised intestinal mucosa, heightened permeability of the intestinal barrier, and facilitate the translocation of gut microbiota metabolites to the liver, thereby exacerbating liver injury (Safari and Gerard, 2019). The composition of the gut microbiota is dynamic and intricately influenced by factors such as age, environment, and dietary patterns. Individuals with NAFLD, as well as animals with similar conditions, exhibit shifts in the species composition and functional traits of gut microbiota. These changes are often characterized by an increased F/B ratio, a decline in beneficial species, and an augmentation of pathogenic bacteria (Gupta et al., 2021). The present study also observed changes such as a decrease in *Bacteroides* abundance. *Bacteroides* has attracted much attention due to its potential regulatory role in liver disease. In recent years, numerous studies have concentrated on the impact of *Bacteroides* when isolated from the host and reintroduced into the host system, with the aim of understanding their potential in ameliorating liver diseases. For instance, Wang et al. (2022) isolated *Bacteroides acidificans* from mouse feces, demonstrating its ability to enhance liver antioxidant capacity by reducing the ratio of L-glutathione/glutathione, thereby modulating the CD95/CD95L signaling pathway to alleviate canavalin-induced liver injury. Furthermore, *Bacteroides uniformis* and *Bacteroides xylanisolvens*, along with other *Bacteroides* species, have been reported to confer beneficial effects in NAFLD (Lee et al., 2021; Qiao et al., 2020). In our study, *B. fragilis* was isolated from the cecum of laying hens and administered to laying hens with diet-induced FLHS resulting from the HELP diet.

The liver serves as the primary site for lipid metabolism in laying hens, bearing almost all synthetic pressure. During egg production in laying hens, over 50% of the fat synthesized in the liver is transported to the ovaries for the formation of egg yolks. The increased demand for egg production exacerbates the metabolic pressure on the liver. Under normal circumstances, hepatic lipid metabolism is in dynamic equilibrium. However, external factors such as increased energy intake and reduced levels of antioxidants in the diet can lead to oxidative stress, disrupting hepatic lipid metabolism and transport, resulting in hepatic lipid deposition, ultimately leading to FLHS (Attallah et al., 2022). In the study by Attallah et al. (2022), HELP feed could induce oxidative stress, leading to liver cell membrane damage and hepatic lipid degeneration in laying hens with FLHS. Similar observations were observed in our study. Pathological results showed severe hepatic steatosis in the HELP group, which was significantly ameliorated by *B. fragilis* intervention. Liver damage associated with oxidative stress is often accompanied by membrane damage, as evidenced by elevated AST and ALT levels in blood of laying hens. However, *B. fragilis* intervention could alleviate liver damage caused by oxidative stress and maintain liver function. Additionally, liver damage was accompanied by enhanced gluconeogenesis (Lee et al., 2021), leading to the conversion of non-carbohydrate substances such as proteins into glucose. This resulted in decreased levels of lipoproteins, affecting the process of lipid transport, ultimately leading to a decline in egg production. The improvement in liver damage by *B. fragilis* contributed to the attenuation of gluconeogenesis in FLHS-affected laying hens, which has a positive effect on maintaining blood glucose and protein levels. Additionally, excess glucose was
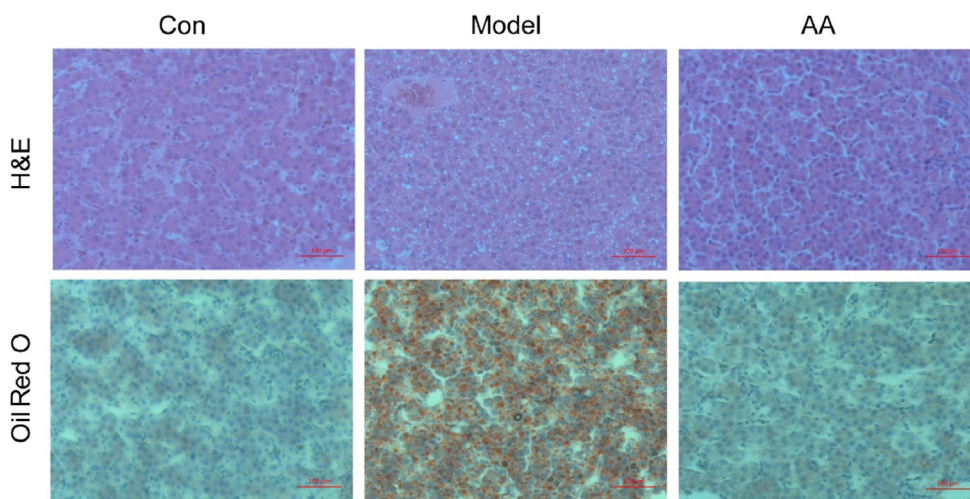

Fig. 8. Arachidonic acid (AA) improved hepatic lipid deposition induced by the high-energy and low-protein diet. Hematoxylin and eosin (H&E) staining, and Oil Red O staining. The scale bar on the figure is 100 μm. Con = control group, hens fed with standard diet; Model = model group, hens fed with high-energy low-protein diet; AA = experimental groups, hens fed with high-energy low-protein diet with 0.3% AA.

Table 8
AA improved blood lipids and liver function in serum[1].

Item	Con	Model	AA	P-value
TG, mmol/L	17.23 ± 1.412[b]	30.25 ± 1.128[a]	16.18 ± 1.358[b]	<0.001
TC, mmol/L	2.87 ± 0.132[b]	4.11 ± 0.362l[a]	2.87 ± 0.188[b]	0.004
LDL-C, mmol/L	0.75 ± 0.086[b]	1.11 ± 0.085[a]	0.73 ± 0.063[b]	0.005
HDL-C, mmol/L	0.92 ± 0.060[a]	0.66 ± 0.044[b]	0.87 ± 0.092[ab]	0.039
AST, U/L	146.00 ± 3.719[b]	176.00 ± 3.844[a]	144.00 ± 4.983[b]	0.003
ALT, U/L	5.40 ± 0.376[ab]	6.65 ± 0.391[a]	5.17 ± 0.360[b]	0.029

AA = arachidonic acid; TG = triglyceride; TC = total cholesterol; HDL-C = high density lipoprotein cholesterol; LDL-C = low density lipoprotein cholesterol; AST = aspartate aminotransferase; ALT = alanine aminotransferase.
[a,b]Mean values within a row with different superscript letters indicate significant difference ($P < 0.05$). Values are means ± SEM, $n = 6$.
[1] Con = control group, hens fed with standard diet; Model = model group, hens fed with high-energy low-protein diet; AA = experimental groups, hens fed with high-energy low-protein diet with 0.3 % AA.

converted into fat for storage, but in FLHS-affected laying hens treated with *B. fragilis*, fat levels remained normal. Therefore, it is speculated that *B. fragilis* might enhance the assimilation or oxidation process of glucose in the liver to meet the energy requirements necessary for production. However, research on the effects of *B. fragilis* on hepatic glucose metabolism has not been conducted and requires further investigation for confirmation.

The restoration of liver function also contributes to maintaining normal lipid metabolism processes. The study results showed that *B. fragilis* intervention significantly reduced TG levels, indicating that this bacterium might improve processes such as TG absorption, transport, and synthesis. This result was also confirmed in another study, where *B. fragilis* supernatant significantly reduced TG levels in liver cells (Li et al., 2023). Additionally, improvements in TC levels
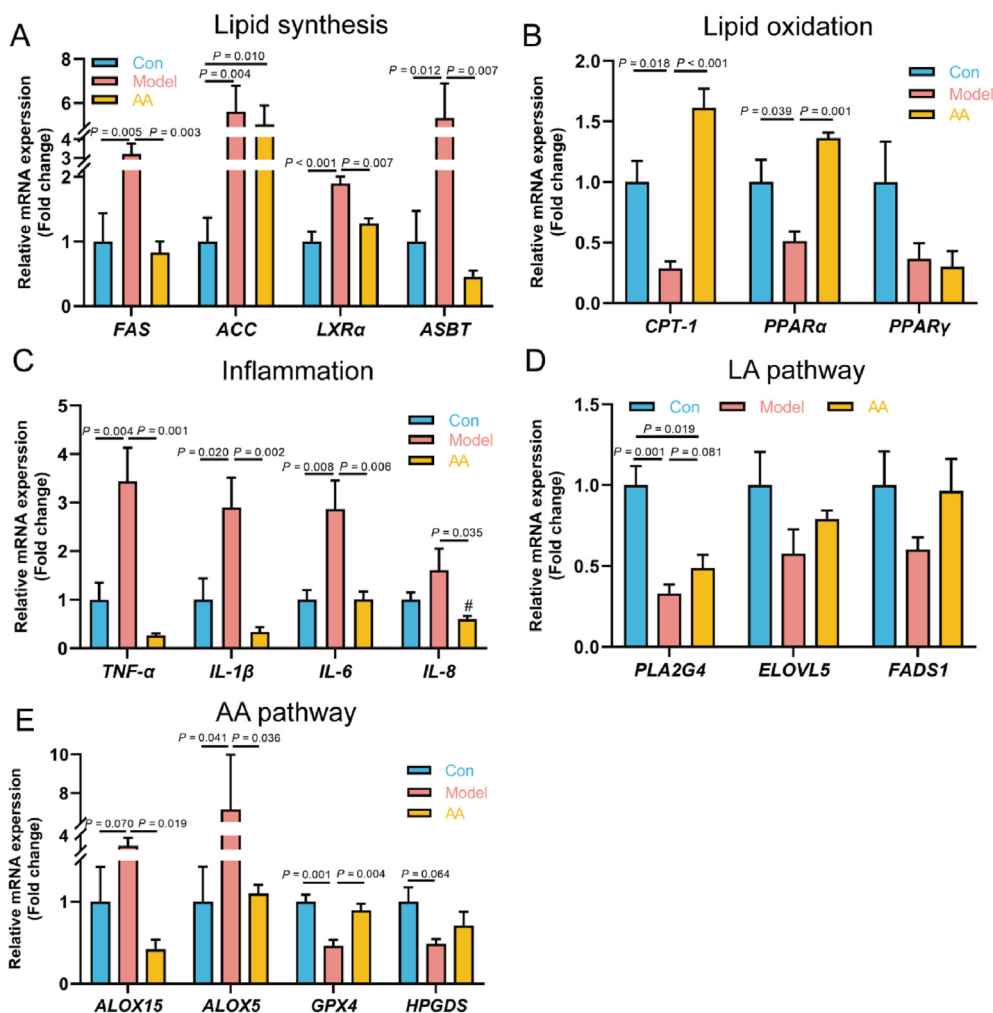

Fig. 9. The impact of arachidonic acid (AA) on gene expression in the liver from laying hens with fatty liver hemorrhagic syndrome. Relative mRNA expression of (A) lipid synthesis, (B) lipid oxidation, (C) inflammation, (D) the linoleic acid (LA) metabolic pathway, and (E) the AA metabolic pathway. Con = control group, hens fed with standard diet; Model = model group, hens fed with high-energy low-protein diet; AA = experimental groups, hens fed with high-energy low-protein diet with 0.3% AA; FAS = fatty acid synthase; ACC = acetyl-CoA carboxylase; LXRα = liver X receptor α; ASBT = apical sodium-dependent bile acid transporter; PPAR = peroxisome proliferator activated receptor; CPT-1 = carnitine palmitoyl transferase-1; TNF-α = tumor necrosis factor-α; IL = interleukin; PLA2G4 = phospholipase A2 group IVA; ELOVL5 = elongase of very-long fatty acid 5; FADS1 = fatty acid desaturase 1; ALOX15 = arachidonate 15-lipoxygenase; ALOX5 = arachidonate 5-lipoxygenase; GPX4 = glutathione peroxidase 4; HPGDS = hematopoietic prostaglandin D synthase. Values are presented as means ± SEM ($n = 5$). When $P < 0.05$, the difference between the two groups is significant.

were observed with *B. fragilis* intervention. This might be related to inherent ability of *B. fragilis* to degrade TC (Li et al., 2023), resulting in a reduction in TC content entering the bloodstream or liver at the source. Furthermore, the elevation of HDL-C levels also contributes to lowering TC levels. This is because HDL-C can transport TC from extrahepatic tissues to the liver for metabolism, converting it into bile acids for excretion. Increased TC levels in FLHS-affected laying hens can lead to an increase in LDL-C levels, as LDL-C is an important carrier of TC. Due to the increased free radicals and decreased antioxidants in FLHS-affected laying hens, LDL-C was highly susceptible to oxidation. Oxidized LDL-C deposited in blood vessels, making it difficult to transport to the liver for degradation or to be used in egg production. However, inherent antioxidative capacity of *B. fragilis* (Li et al., 2023) helped protect LDL-C from oxidation and facilitated the transport of lipids to eggs. The antioxidative capacity of *B. fragilis* also contributed to protecting the nutrients in the feed from oxidation, thereby ensuring their absorption by FLHS-affected laying hens and meeting the nutritional needs for egg production.

To delve deeper, we employed RT-PCR to analyze the influence of *B. fragilis* on gene expression, particularly focusing on genes associated with lipid metabolism, lipid oxidation, and inflammatory factors, which are pivotal in the context of hepatic steatosis. Within the realm of lipid metabolism, ACC emerges as the pivotal rate-limiting enzyme for de novo fatty acid synthesis (Batchuluun et al., 2022). In the cytoplasm, ACC generates malonyl-CoA, a precursor for fatty acid synthesis. FAS orchestrates the actual synthesis of fatty acids. Meanwhile, ACC2 is located on the outer mitochondrial membrane and produces a product that inhibits CPT-1. This inhibition suppresses fatty acid oxidation in the mitochondria. LXRα promotes hepatic cholesterol metabolism and induces the synthesis of proteins such as sterol regulatory element binding protein-1c, FAS, and stearoyl-CoA desaturase 1, thereby facilitating lipid synthesis (Wang and Tontonoz, 2018). Additionally, ASBT participates in triglyceride and cholesterol synthesis by influencing the transcription of sterol regulatory element binding protein 1c (Li et al., 2020). PPARα, which is highly expressed in the liver, primarily promotes fatty acid oxidation (Devan et al., 2022). In our investigation, the administration of *B. fragilis* to laying hens precipitated a notable decline in the expression of genes linked to hepatic lipid synthesis, while the expression of genes associated with lipid oxidation significantly increased. This may be the direct way *B. fragilis* improve FLHS. Dysregulated lipid metabolism cause by increase energy in the diet culminates in excessive hepatic lipid accumulation and steatosis, thereby heightening susceptibility to damage stemming from inflammation (Peiseler et al., 2022). Consequently, inflammation is a crucial player in the progression of NAFLD. Inflammatory gene expression showcased a substantial elevation in the expression of inflammatory cytokines (*TNF-α*, *IL-1β*, and *IL-6*) in chickens afflicted with hepatic lipidosis. However, this elevation was significantly alleviated following *B. fragilis* intervention, underscoring the significant role of *B. fragilis* in mitigating liver inflammation. These findings are consistent with prior reports detailing its anti-inflammatory effects (Chang et al., 2019). In summary, these findings underscore the potential of *B. fragilis* in ameliorating hepatic lipidosis, rendering it a plausible therapeutic candidate for addressing FLHS and related metabolic disorders.

B. fragilis, a model strain of the *Bacteroides* genus, plays a pivotal role in modulating gut microbiota. While *B. fragilis* did not markedly alter the diversity of the gut microbiota, it did induce shifts in its composition. At the phylum level, *B. fragilis* significantly reduced the relative abundance of Proteobacteria. Proteobacteria, a gram-negative bacteria characterized by lipopolysaccharide-rich outer membranes, encompass numerous pathogens. Multiple studies have indicated that Proteobacteria exhibit a notable increase in the gut of NAFLD patients, linked to hepatic inflammation, which

subsequently significantly decreases after pharmacological interventions (Ran et al., 2022; Sookoian et al., 2020; Yang et al., 2022). At the genus level, *B. fragilis* intervention resulted in a highly significant increase in the relative abundance of *Bacteroides*, along with a tendency toward elevated levels of *Monoglobus* and *Clostridiales DTU089*. Furthermore, *B. fragilis* intervention also drastically decreased the relative abundance of *Succinatimonas* and *Faecalicoccus*. *Bacteroides* thrives in the cecum of laying hens and has been shown to confer beneficial effects in improving NAFLD. Tsai et al. (2020) revealed reduced levels of Clostridiales in the feces of NAFLD and NASH patients compared to healthy individuals. Similarly, in another study, the levels of Clostridiales increased in NAFLD mice after treatment with defatted walnut powder extract (Ren et al., 2021). This suggests that Clostridiales may play a role in counteracting NAFLD development to some extent. Like Clostridiales, *Monoglobus* is enriched in healthy individuals and diminished in those with liver disease (Li et al., 2022). *Succinatimonas* has been reported to efficiently metabolize carbohydrates, positively correlating with most carbohydrate metabolic pathways (Xue et al., 2022). In animals with NAFLD, an elevated relative abundance of this bacterium implies increased host energy intake. By lowering the relative abundance of *Succinatimonas*, *B. fragilis* may also reduce the associated energy intake, potentially benefiting NAFLD. Additionally, through correlation analysis, it was found that the elevated bacteria due to *B. fragilis* intervention (*Bacteroides* and *Clostridiales DTU089*) exhibited significant negative correlations with TG, TC, and LDL-C levels. Conversely, decreased *Faecalicoccus* was negatively correlated with these indicators. This suggests that the differential bacterial species altered by *B. fragilis* contribute to alleviating blood lipid levels. Furthermore, KEGG enrichment analysis also indicated that *B. fragilis* intervention significantly decreased NAFLD-related metabolic pathways. However, the relationship between *B. fragilis* and changes in the gut microbiota requires further exploration.

NAFLD progression is often accompanied by chronic low-grade inflammation (Scorletti and Carr, 2022), a point corroborated in our aforementioned research. Bioactive eicosanoids and oxylipins play a pivotal role in liver damage, inflammation, and other metabolic disorders (Alba et al., 2023). Thus, to further elucidate the mechanism by which *B. fragilis* improved hepatic inflammation and lipid metabolism, we employed targeted lipidomics to assess variations in various oxylipins within the liver. Under the influence of *B. fragilis*, OPLS-DA of hepatic samples revealed distinct separation in oxylipin profiles, suggesting perturbation in their metabolic profile. Moreover, we identified twelve differential metabolites and conducted gene expression analysis on key genes within selected metabolic pathways. The levels of AA, LA, and D-γ-LA are substantial, and as substrates for oxylipin metabolism pathways, they exert a significant influence on oxylipin metabolism. Therefore, analysis of these three substances was also conducted. Under the influence of PLA2G4, LA is released from phospholipids, and subsequently desaturated to generate γ-LA, which is then converted to D-γ-LA via ELOVL5, ultimately leading to AA through desaturation catalyzed by FADS1 (Mustonen and Nieminen, 2023). Following *B. fragilis* intervention, the contents of LA, D-γ-LA, and AA all showed significant increases. Notably, the expression of related genes in this pathway exhibited an upward trend but was not statistically significant, potentially due to alternative pathways mediating the observed increases in LA and AA content. AA, one of the essential n-6 fatty acids, generates a range of prostaglandins and LTBs, serving as highly active inflammatory mediators involved in various processes such as inflammation, lipid metabolism, and energy homeostasis (Monteiro et al., 2014). In previous studies, including our own, AA levels have been observed to decrease under high-fat dietary conditions (Meng et al., 2021; Shi et al., 2023). For

instance, Shi et al. (2023) demonstrated that the addition of pomegranate peel polyphenols to the diet improved NAFLD and led to an increase in AA content in mice. In alignment with these findings, our study revealed that while the HELP diet significantly decreased AA levels in the liver, B. fragilis intervention effectively reversed this alteration.

The differential metabolites within the AA metabolic pathway, including 15-keto-PGE$_2$, 15-oxoETE, and 12-oxoETE, were significantly downregulated by B. fragilis. Of note, 15-keto-PGE$_2$ is a product of PGE$_2$ inactivation, partially substituting and terminating the inflammatory response mediated by PGE$_2$ (Endo et al., 2020). However, in our investigation, B. fragilis led to a reduction in the level of this substance. This molecule has been reported to activate PPARγ, contributing to enhanced fatty acid oxidation and anti-inflammatory effects (Lu et al., 2014). However, under the influence of the HELP diet, the expression of hepatic inflammatory genes in chickens was elevated, and PPARγ gene expression exhibited a declining trend. The landscape of hepatic lipid metabolism is intricate, with NAFLD arising from the interplay of multiple factors. In our study, the HELP diet triggered hepatic inflammation and lipidosis, potentially stemming from other factors. The levels of proinflammatory substances, such as 15-oxoETE and 12-oxoETE, increased under the influence of the HELP diet but were significantly reduced after B. fragilis intervention. Additionally, the expression of the GPX4 gene, which is crucial in maintaining lipid redox homeostasis (X Gao et al., 2021), was significantly elevated by B. fragilis. This aligns with findings from Zhan et al. (2022), where substances such as 15-oxoETE, induced by lipopolysaccharides and D-galactosamine, were reduced upon oridonin intervention, accompanied by diminished expression of genes such as ALOX12, ALOX5, and ALOX15, mirroring our study. Furthermore, the content of PGD$_2$, an AA metabolite, was notably reduced by the HELP diet, while B. fragilis intervention led to a slight increase, albeit not statistically significant. PGD$_2$ has been reported to possess anti-inflammatory properties and contribute to lipid metabolism regulation, primarily by enhancing insulin sensitivity (Le Loupp et al., 2015). However, some reports indicate its potential negative impact on lipid metabolism (Wang et al., 2021). In the context of the LA metabolic pathway, ALOX15 catalyzes the conversion of LA to 13(S)-HpODE, ultimately resulting in 13-oxoODE. Notably, the gene expression level of ALOX15 in our study aligned with the content level of 13(S)-HpODE. 13(S)-HpODE and 13-oxoODE are endogenous ligands of PPARγ, contributing to inflammatory and lipid oxidation processes (Biswas et al., 2023). In this study, intervention by B. fragilis led to a reduction in the levels of both compounds, suggesting that B. fragilis might improve oxylipin metabolism by modulating the ALOX15 pathway. In the context of the correlation analysis between clinical indicators and metabolites, significant negative correlations were observed between AA, LA, D-γ-LA, and TG, TC, LDL-C levels, implying their pivotal role in lipid profile improvement.

In the aforementioned study, we explored the impact of B. fragilis on the gut microbiota and oxylipins; however, the relationship between these two factors remains elusive. Thus, we conducted a joint analysis of the changes induced by B. fragilis in hepatic oxylipins and differential bacterial species. The results revealed a highly significant positive correlation between Bacteroides and AA, with both exhibiting the highest relative abundance and substance content in their respective domains. Additionally, B. fragilis in vitro culture experiments confirmed its ability to produce AA, a phenomenon also observed in the research conducted by other studies (Yan et al., 2020). Therefore, we speculate that B. fragilis might improve FLHS by secreting AA. The potential benefits of supplementing AA in the diet to mitigate obesity, NAFLD, or other metabolic disorders are subject to some controversy. On one hand, reports suggest that AA might have detrimental effects on

NAFLD, possibly serving as an indicator of hepatic inflammation (Monteiro et al., 2014; Sztolsztener et al., 2020). On the other hand, AA can enhance blood lipid profiles, and fatty acid metabolism, and regulate gut microbiota to exert anti-NAFLD effects. Zhuang et al. (2017) observed gender-related differences in the effectiveness of AA supplementation for NAFLD when added to a high-fat diet. Further investigations revealed that AA can influence the gut microbiota in a sex-dependent manner, ameliorating microbiota-driven low-grade inflammation and improving NAFLD through the gut−brain−liver axis. In our study, we confirmed the potential of AA to ameliorate FLHS by supplementing it in cell culture media and animal diets. The cellular results demonstrated AA's direct impact on liver cells, lowering TG and LDL-C levels in chicken LMH cells. In animal experiments, AA also exhibited a positive effect on improving FLHS, primarily manifesting as mitigated increases in body and liver weight induced by the HELP diet, changes in blood lipids, and liver pathology and function alterations. These findings align with the positive effects of B. fragilis intervention on FLHS. Gene expression analysis revealed that AA enhanced the expression of genes related to hepatic lipid synthesis, fatty acid oxidation, and inflammation, closely resembling the effects of B. fragilis. Further RT-PCR analysis of genes involved in oxylipin metabolism pathways demonstrated that the changes in gene expression caused by AA were consistent with the trends seen with B. fragilis intervention (Fig. 9). This suggests that AA exerts its anti-FLHS effects by ameliorating clinical indicators, lipid metabolism, inflammation, and oxylipin metabolism disruption, much like the effects of B. fragilis. Therefore, the ameliorative effect of B. fragilis on FLHS is closely related to its metabolic product AA.

5. Conclusions

In conclusion, B. fragilis had the capacity to improve FLHS by altering the composition of the gut microbiota and modulating oxylipin metabolism, with AA playing a crucial role. This study extends our understanding of the impact of B. fragilis on HELP diet-induced FLHS in laying hens, encompassing improvements in blood lipids, lipid metabolism, inflammation, gut microbiota, and oxylipin metabolism, as well as their interrelationships. Furthermore, this study validated the beneficial effects of the B. fragilis metabolite AA on FLHS through in vivo and in vitro experiments. B. fragilis might exert its anti-FLHS effects through its metabolite AA. Nevertheless, we have not conducted further validation by knocking out the gene responsible for AA production in B. fragilis. As such, the exact mechanisms through which B. fragilis exerts its effects warrant further exploration.

CRediT authorship contribution statement

Shaobo Zhang: Formal analysis, Investigation, Methodology, Visualization, Writing − original draft. **Manhua You:** Formal analysis, Investigation, Validation. **Youming Shen:** Formal analysis, Software, Visualization. **Xinghua Zhao:** Data curation, Methodology, Writing − review & editing. **Xin He:** Resources, Writing − review & editing. **Juxiang Liu:** Resources, Writing − review & editing. **Ning Ma:** Conceptualization, Funding acquisition, Project administration, Supervision.

Availability of data and materials

The datasets used during the current study are available from the corresponding author on reasonable request. The datasets of intestinal flora sequencing generated during the current study are available in the NCBI repository, National Center for Biotechnology Information (nih.gov), with the bioproject number PRJNA1021533.

Declaration of competing interest

We declare that we have no financial and personal relationships with other people or organizations that can inappropriately influence our work, and there is no professional or other personal interest of any nature or kind in any product, service and/or company that could be construed as influencing the content of this paper.

Acknowledgements

Appendix supplementary data

Supplementary data to this article can be found online at https://doi.org/10.1016/j.aninu.2024.08.008.

References

Alba MM, Ebright B, Hua B, Slarve I, Zhou Y, Jia Y, et al. Eicosanoids and other oxylipins in liver injury, inflammation and liver cancer development. Front Physiol 2023;14:1098467.

Attallah OK, Mohammed TT, Al-Anbari NN. Effect of adding grape pomace and resveratrol on some physiological traits and gene expression to prevent hemorrhagic fatty liver syndrome in laying hens. IOP Conf Ser Earth Environ Sci 2022;1060:012076.

Barquissau V, Ghandour RA, Ailhaud G, Klingenspor M, Langin D, Amri EZ, et al. Control of adipogenesis by oxylipins, GPCRs and PPARs. Biochimie 2017;136:3–11.

Batchuluun B, Pinkosky SL, Steinberg GR. Lipogenesis inhibitors: therapeutic opportunities and challenges. Nat Rev Drug Discov 2022;21:283–305.

Biswas P, Swaroop S, Dutta N, Arya A, Ghosh S, Dhabal S, et al. IL-13 and the hydroperoxy fatty acid 13(S)HpODE play crucial role in inducing an apoptotic pathway in cancer cells involving MAO-A/ROS/p53/p21 signaling axis. Free Radic Biol Med 2023;195:309–28.

Byrne CD, Targher G. NAFLD: a multisystem disease. J Hepatol 2015;62(Suppl 1): S47–64.

Chang CJ, Lin TL, Tsai YL, Wu TR, Lai WF, Lu CC, et al. Next generation probiotics in disease amelioration. J Food Drug Anal 2019;27:615–22.

Chen C, Liao J, Xia Y, Liu X, Jones R, Haran J, et al. Gut microbiota regulate Alzheimer's disease pathologies and cognitive disorders via PUFA-associated neuroinflammation. Gut 2022;71:2233–52.

Devan AR, Nair B, Kumar AR, Nath LR. An insight into the role of telmisartan as PPAR-gamma/alpha dual activator in the management of nonalcoholic fatty liver disease. Biotechnol Appl Biochem 2022;69:461–8.

Endo S, Suganami A, Fukushima K, Senoo K, Araki Y, Regan JW, et al. 15-Keto-PGE (2) acts as a biased/partial agonist to terminate PGE (2)-Evoked signaling. J Biol Chem 2020;295:13338–52.

Gai Z, Visentin M, Gui T, Zhao L, Thasler WE, Häusler S, et al. Effects of farnesoid X receptor activation on arachidonic acid metabolism, NF-kB signaling, and hepatic inflammation. Mol Pharmacol 2018;94:802–11.

Gao G, Xie ZS, Li EW, Yuan Y, Fu Y, Wang P, et al. Dehydroabietic acid improves nonalcoholic fatty liver disease through activating the Keap1/Nrf2-ARE signaling pathway to reduce ferroptosis. J Nat Med 2021;75:540–52.

Gao X, Liu S, Ding C, Miao Y, Gao Z, Li M, et al. Comparative effects of genistein and bisphenol a on non-alcoholic fatty liver disease in laying hens. Environ Pollut 2021;288:117795.

Gupta M, Krishan P, Kaur A, Arora S, Trehanpati N, Singh TG, et al. Mechanistic and physiological approaches of fecal microbiota transplantation in the management of NAFLD. Inflamm Res 2021;70:765–76.

Hamid H, Zhang JY, Li WX, Liu C, Li ML, Zhao LH, et al. Interactions between the cecal microbiota and non-alcoholic steatohepatitis using laying hens as the model. Poultry Sci 2019;98:2509–21.

Le Loupp AG, Bach-Ngohou K, Bourreille A, Boudin H, Rolli-Derkinderen M, Denis MG, et al. Activation of the prostaglandin D2 metabolic pathway in Crohn's disease: involvement of the enteric nervous system. BMC Gastroenterol 2015;15:112.

Lee H, Do M, Jhun H, Ha S, Song H, Roh S, et al. Amelioration of hepatic steatosis in mice through Bacteroides uniformis CBA7346-mediated regulation of high-fat diet-induced insulin resistance and lipogenesis. Nutrients 2021;13:2989.

Li M, Wang Q, Li Y, Cao ST, Zhang YJ, Wang ZQ, et al. Apical sodium-dependent bile acid transporter, drug target for bile acid related diseases and delivery target for prodrugs: current and future challenges. Pharmacol Ther 2020;212:107539.

Li RX, Yi XZ, Yang JH, Zhu Z, Wang YF, Liu XM, et al. Gut microbiome signatures in the progression of hepatitis B virus-induced liver disease. Front Microbiol 2022;13:916061.

Li S, Yan C, Liu T, Xu C, Wen K, Liu L, et al. Research note: increase of bad bacteria and decrease of good bacteria in the gut of layers with vs. without hepatic steatosis. Poultry Sci 2020;99:5074–8.

Li X. Isolation and identification of Bacteroides fragilis and its functional properties. Shenyang Agricultural University; 2023 [Master Degree Thesis Dissertation].

Liu X, Pan YC, Shen YM, Liu HL, Zhao XH, Li JY, et al. Protective effects of Abrus cantoniensis hance on the fatty liver hemorrhagic syndrome in laying hens based on liver metabolomics and gut microbiota. Front Vet Sci 2022;9:862006.

Lu D, Han C, Wu T. 15-PGDH Inhibits hepatocellular carcinoma growth through 15-keto-PGE (2)/PPAR gamma-mediated activation of P21 (WAF1/Cip 1). Oncogene 2014;33:1101–12.

Meng J, Ma N, Liu H, Liu J, Liu J, Wang J, et al. Untargeted and targeted metabolomics profiling reveals the underlying pathogenesis and abnormal arachidonic acid metabolism in laying hens with fatty liver hemorrhagic syndrome. Poultry Sci 2021;100:101320.

Monteiro J, Leslie M, Moghadasian MH, Arendt BM, Allard JP, Ma D. The role of n-6 and n-3 polyunsaturated fatty acids in the manifestation of the metabolic syndrome in cardiovascular disease and non-alcoholic fatty liver disease. Food Funct 2014;5:426–35.

Mustonen AM, Nieminen P. Dihomo-gamma-Linolenic acid (20:3n-6)-metabolism, derivatives, and potential significance in chronic inflammation. Int J Mol Sci 2023;24:2116.

Peiseler M, Schwabe R, Hampe J, Kubes P, Heikenwalder M, Tacke F. Immune mechanisms linking metabolic injury to inflammation and fibrosis in fatty liver disease - novel insights into cellular communication circuits. J Hepatol 2022;77: 1136–60.

Purba DR. Effect of Dietary supplementation of arachidonate acid (ARA) oil and vitamin E on production performance, egg quality, fatty acid composition and lipid oxidation in laying hens. Chinese Academy of Agricultural Sciences; 2021 [Master Degree Thesis Dissertation].

Qiao S, Bao L, Wang K, Sun S, Liao M, Liu C, et al. Activation of a specific gut Bacteroides-folate-liver axis benefits for the alleviation of nonalcoholic hepatic steatosis. Cell Rep 2020;32:108005.

Ran X, Hu GQ, He FD, Li KF, Li F, Xu DW, et al. Phytic acid improves hepatic steatosis, inflammation, and oxidative stress in high-fat diet (HFD)-fed mice by modulating the gut-liver axis. J Agric Food Chem 2022;70:11401–11.

Ren SM, Zhang QZ, Chen ML, Jiang M, Zhou Y, Xu XJ, et al. Anti-NAFLD effect of defatted walnut powder extract in high fat diet-induced C57BL/6 mice by modulating the gut microbiota. J Ethnopharmacol 2021;270:113814.

Rohwer N, Jelleschitz J, Hohn A, Weber D, Kuhl AA, Wang C, et al. Prevention of colitis-induced liver oxidative stress and inflammation in a transgenic mouse model with increased omega-3 polyunsaturated fatty acids. Redox Biol 2023;64:102803.

Safari Z, Gerard P. The links between the gut microbiome and non-alcoholic fatty liver disease (NAFLD). Cell Mol Life Sci 2019;76:1541–58.

Scorletti E, Carr R. A new perspective on NAFLD: focusing on lipid droplets. J Hepatol 2022;76:934–45.

Shi HD, Li XZ, Hou C, Chen L, Zhang YH, Li JK. Effects of pomegranate peel polyphenols combined with inulin on gut microbiota and serum metabolites of high-fat-induced obesity rats. J Agric Food Chem 2023;71:5733–44.

Sookoian S, Salatino A, Castano GO, Landa MS, Fijalkowky C, Garaycoechea M, et al. Intrahepatic bacterial metataxonomic signature in non-alcoholic fatty liver disease. Gut 2020;69:1483–91.

Sztolsztener K, Chabowski A, Harasim-Symbor E, Bielawiec P, Konstantynowicz-Nowicka K. Arachidonic acid as an early indicator of inflammation during non-alcoholic fatty liver disease development. Biomolecules 2020;10:1133.

Targher G, Tilg H, Byrne CD. Non-alcoholic fatty liver disease: a multisystem disease requiring a multidisciplinary and holistic approach. Lancet Gastroenterol Hepatol 2021;6:578–88.

Tsai MC, Liu YY, Lin CC, Wang CC, Wu YJ, Yong CC, et al. Gut microbiota dysbiosis in patients with biopsy-proven nonalcoholic fatty liver disease: a cross-sectional study in Taiwan. Nutrients 2020;12:820.

Wang B, Tontonoz P. Liver X Receptors in lipid signalling and membrane homeostasis. Nat Rev Endocrinol 2018;14:452–63.

Wang H, Wang Q, Yang C, Guo M, Cui X, Jing Z, et al. Bacteroides acidifaciens in the gut plays a protective role against CD95-mediated liver injury. Gut Microb 2022;14:2027853.

Wang K, Liao M, Zhou N, Bao L, Ma K, Zheng Z, et al. Parabacteroides distasonis alleviates obesity and metabolic dysfunctions via production of succinate and secondary bile acids. Cell Rep 2019;26:222–35.

Wang W, Zhong X, Guo J. Role of 2-series prostaglandins in the pathogenesis of type 2 diabetes mellitus and non-alcoholic fatty liver disease. Int J Mol Med 2021;47: 114.

Wu GP, Li ZH, Zheng Y, Zhang YH, Liu L, Gong DQ, et al. Supplementing cholamine to diet lowers laying rate by promoting liver fat deposition and altering intestinal microflora in laying hens. Poultry Sci 2022;101:102084.

Xue MY, Xie YY, Zhong Y, Ma XJ, Sun HZ, Liu JX. Integrated meta-omics reveals new ruminal microbial features associated with feed efficiency in dairy cattle. Microbiome 2022;10:32.

Yan XF, Jin JJ, Su XH, Yin XL, Gao J, Wang XW, et al. Intestinal flora modulates blood pressure by regulating the synthesis of intestinal-derived corticosterone in high salt-induced hypertension. Circ Res 2020;126:839–53.

Yang XY, Zheng MX, Zhou ML, Zhou LM, Ge X, Pang N, et al. Lentinan supplementation protects the gut-liver axis and prevents steatohepatitis: the role of gut microbiota involved. Front Nutr 2022;8:803691.

Zhan Z, Zhang T, Dai F, Wen X, Chen Y, Jiang H, et al. Effect of oridonin on oxylipins in the livers of mice with acute liver injury induced by D-galactosamine and lipopolysaccharide. Int Immunopharm 2022;102:108387.

Zhu L, Wang J, Ding X, Bai S, Zeng Q, Xuan Y, et al. Serum trimethylamine-N-oxide and gut microbiome alterations are associated with cholesterol deposition in the liver of laying hens fed with rapeseed meal. Anim Nutr 2021;7:1258–70.

Zhuang P, Shou Q, Lu Y, Wang G, Qiu J, Wang J, et al. Arachidonic acid sex-dependently affects obesity through linking gut microbiota-driven inflammation to hypothalamus-adipose-liver axis. Biochim Biophys Acta, Mol Basis Dis 2017;1863:2715–26.